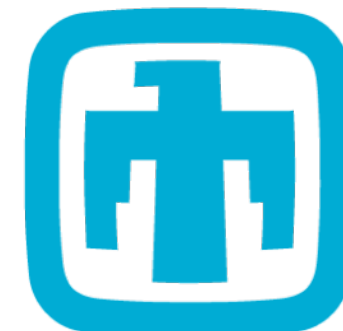


Towards multi-scale modeling of non-LTE: Validation of microscopic models

Andrew Baczewski
Sandia National Laboratories



**Sandia
National
Laboratories**

Multiscale Modeling of Matter under Extreme Conditions
2022-09-14

Sandia National Laboratories is a multimission laboratory managed and operated by National Technology & Engineering Solutions of Sandia, LLC, a wholly owned subsidiary of Honeywell International Inc., for the U.S. Department of Energy's National Nuclear Security Administration under contract DE-NA0003525.

 **CCR**
Center for Computing Research

Acknowledgements

Average-atom methods and calculations:

PI: [Stephanie Hansen \(Sandia\)](#)
[Tommy Hentschel \(Cornell\)](#)

Time-dependent density functional theory calculations:

[Alina Kononov \(Sandia\)](#)

Collision rate/equilibration calculations:

[Brian Robinson \(UIUC\)](#)
[André Schleife \(UIUC\)](#)

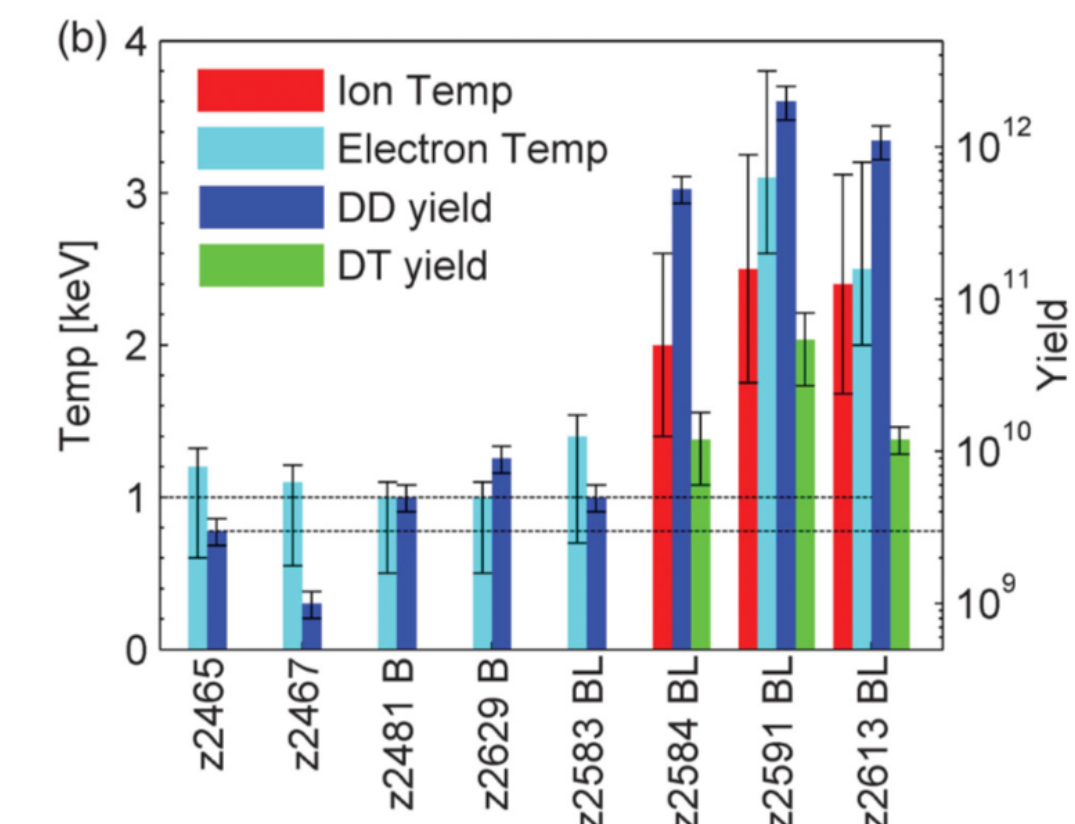
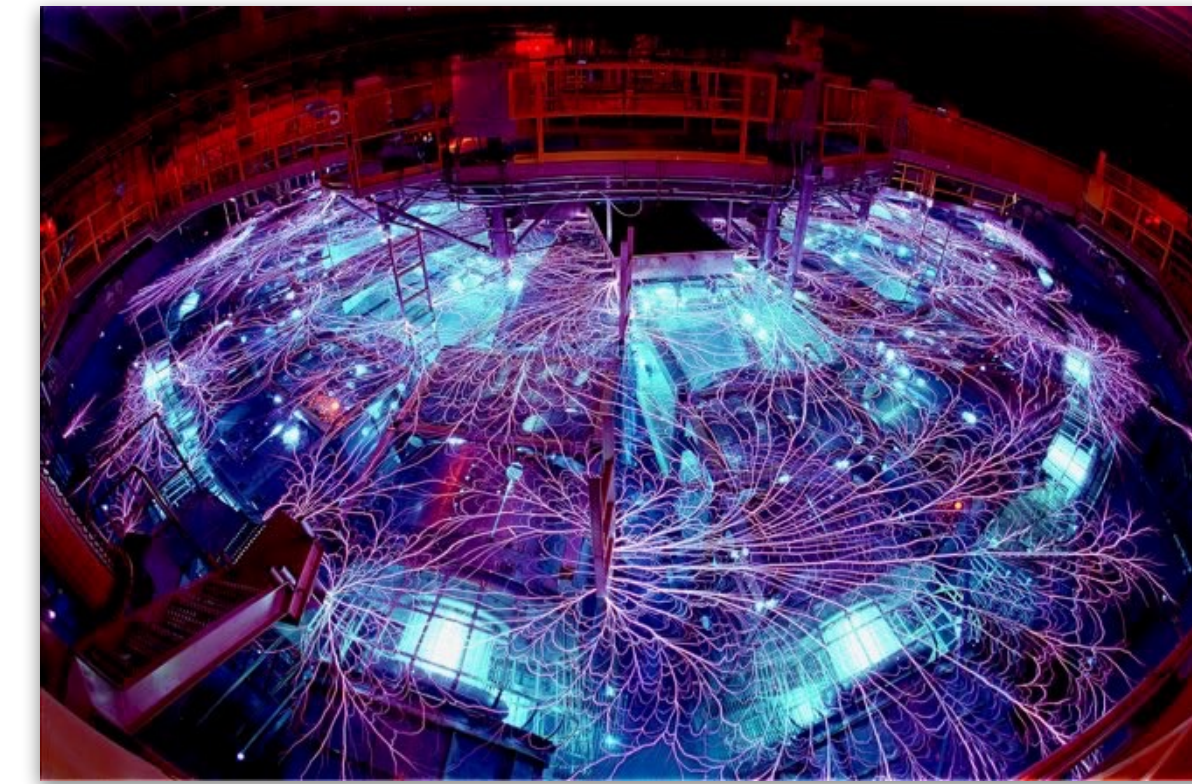
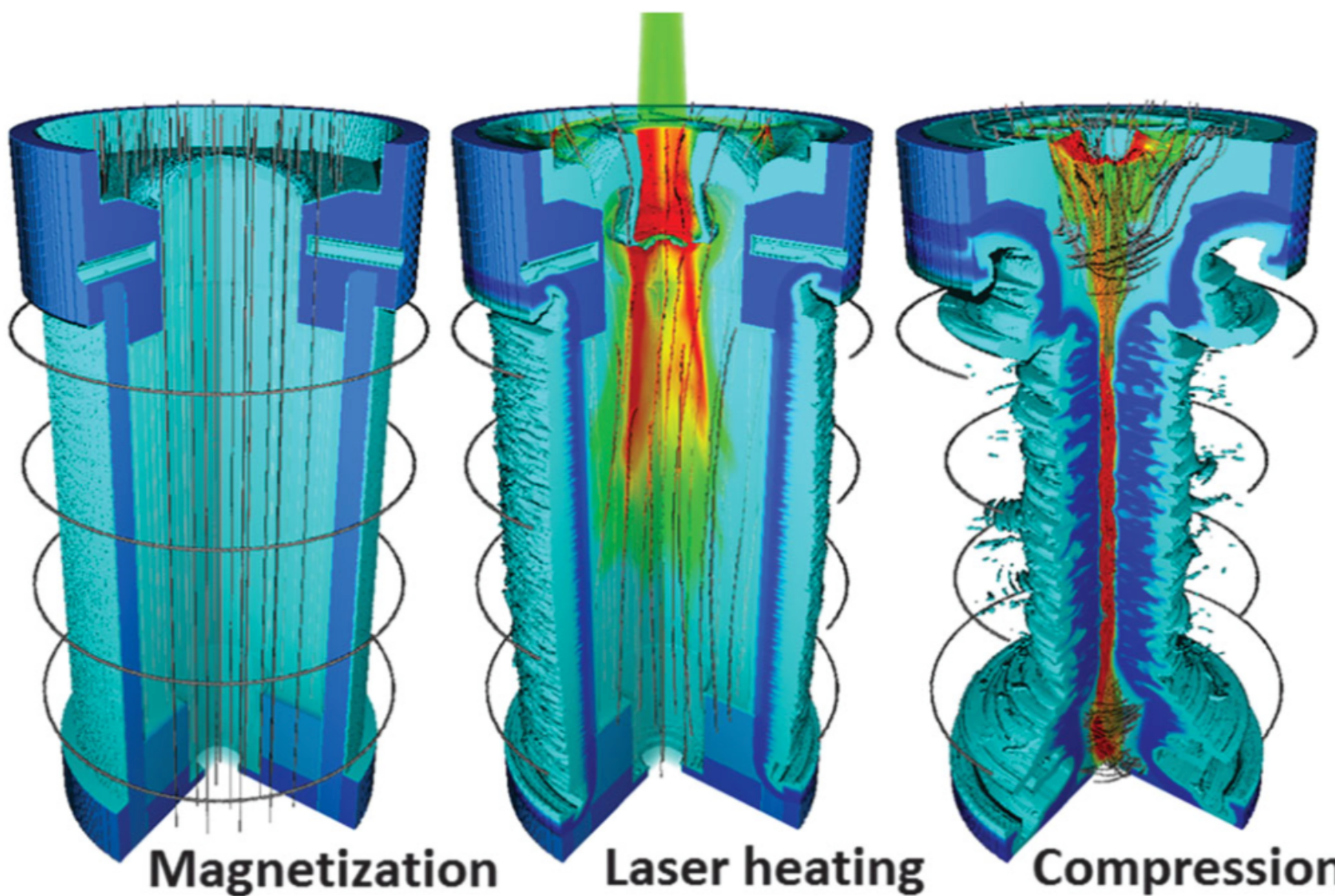
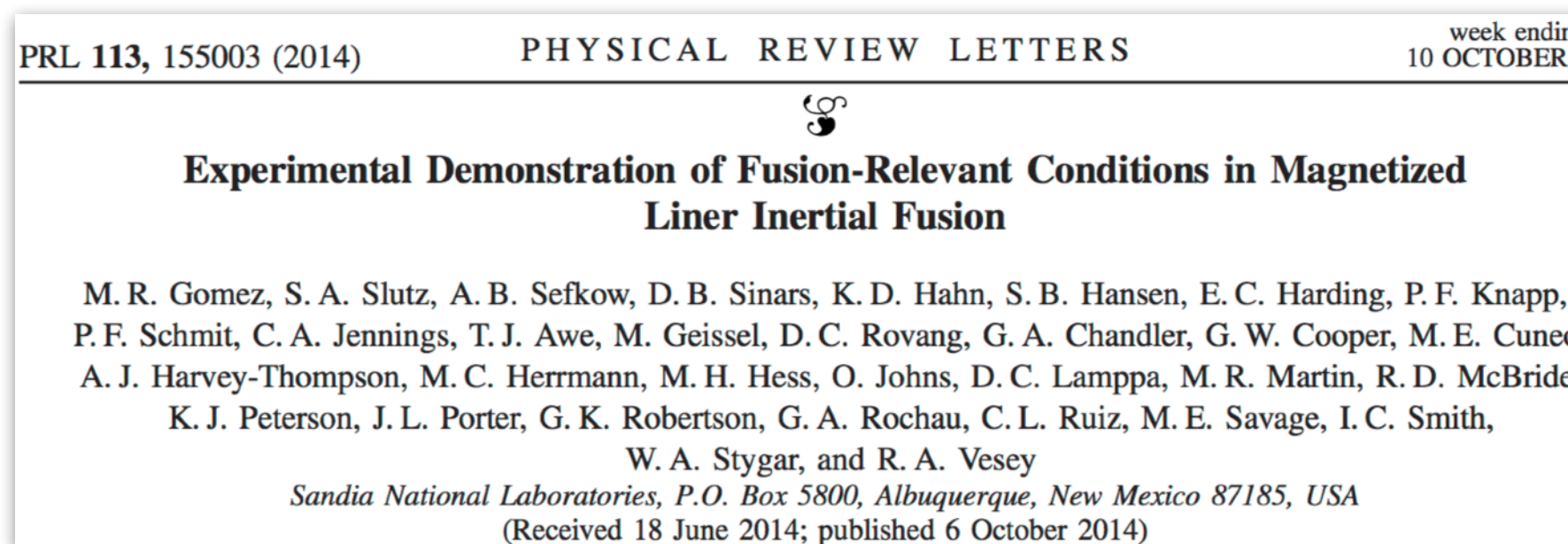
Invaluable conversations:

[Attila Cangi \(CASUS\)](#)
[Kushal Ramakrishnan \(CASUS\)](#)

We are grateful for support from:

[DOE/NNSA](#)
[Sandia LDRD](#)

Experimental design requires wide-ranging models

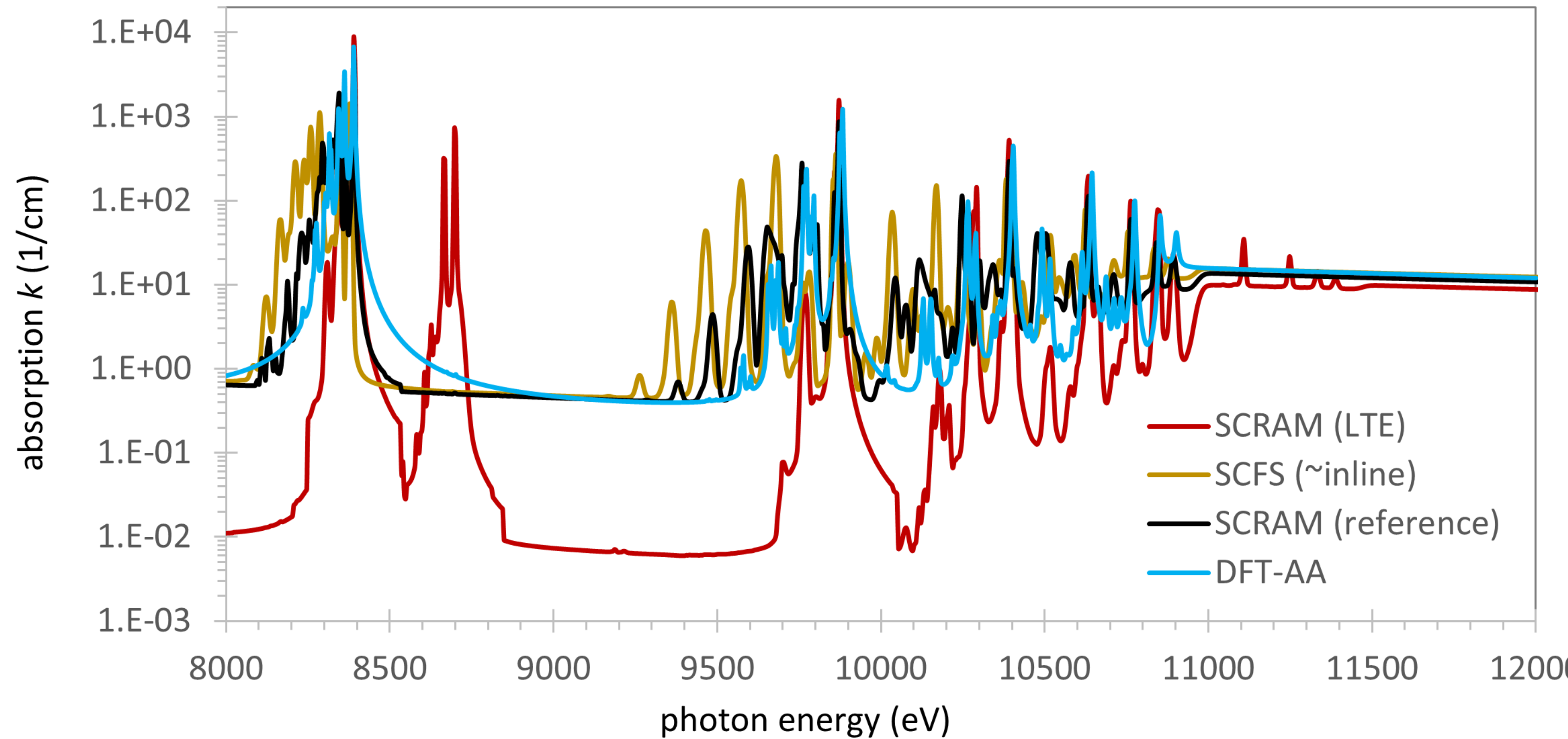


Codes involved in designing experiments like this require materials models

Experimental design requires equation-of-state and transport properties (among many other things)

Densities and temperatures vary over many orders of magnitude, including WDM regime!

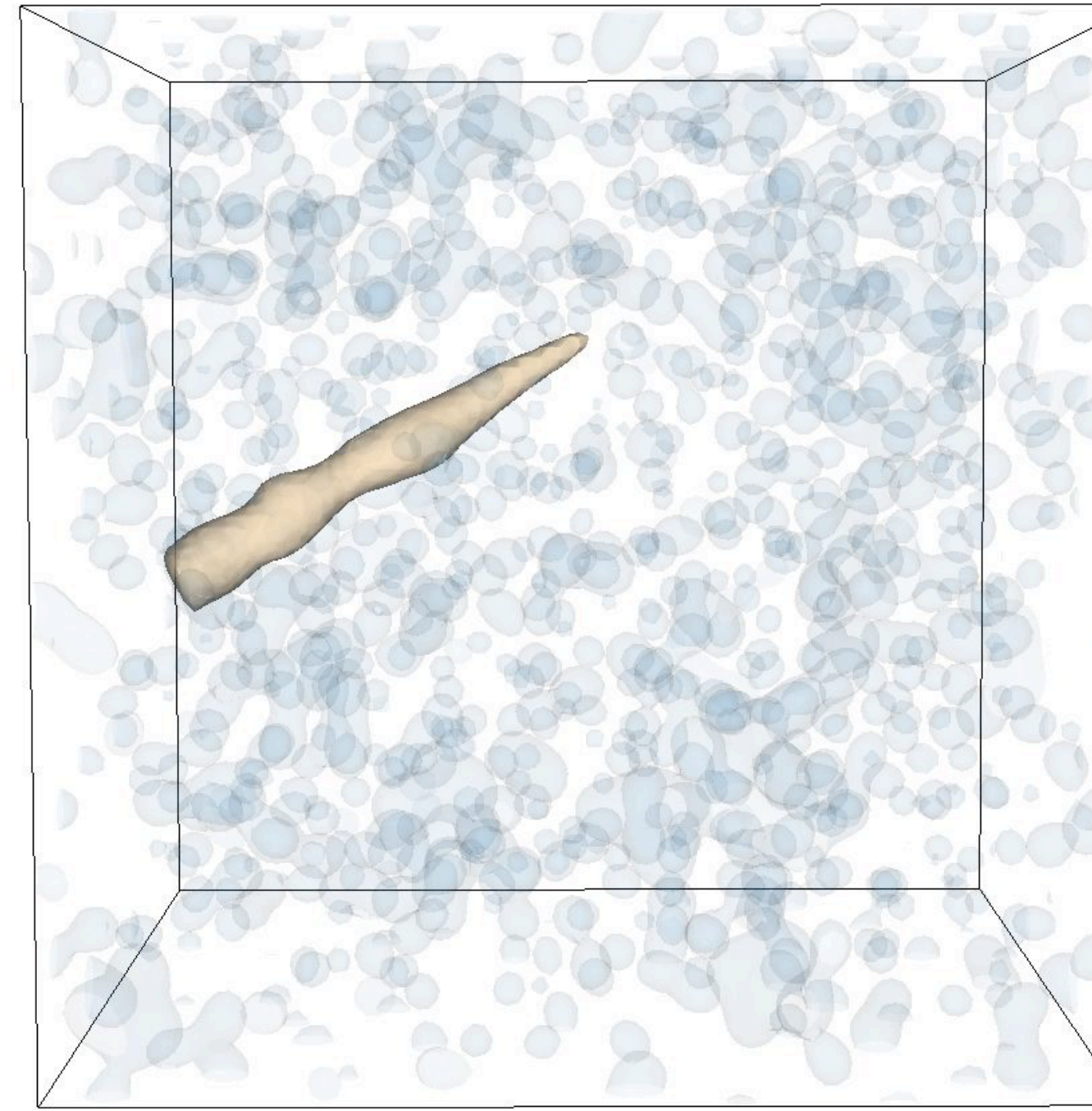
Non-LTE compounds this challenge



(Above) Absorption spectrum for Cu at $T_e=1$ keV, 0.1 g/cm^3
We need codes that can fill out tables to offset the cost of inline models

Many-atom models are expensive

Say that we want to compute electronic stopping power in the fuel...



This calculation consisted of 1024 deuterium atoms, 10 g/cc and 2 eV.

Prepared for the 2016 charged-particle transport coefficient comparison workshop, Grabowski, et al., HEDP, 2020

Each projectile velocity took \sim 1 day on a moderately large HPC system (\sim 10k cores).

Higher Z, higher T, larger cells - all require more time.

Our biggest stopping calculations, 1 curve = 1 machine-week on a million-core system

Average-atom models are inexpensive

We need to cut the cost of these calculations down by **6-8 orders of magnitude*** if we want to use them for tabulation of materials models - particularly non-LTE!

AA models fit this description,

but they're necessarily making more severe approximations than many-atom models.

What does TDDFT tell us about the quality of those approximations?

At Sandia, we've been undertaking a comparison between AA and (TD)DFT methods for a variety of properties - but today I'll primarily be focusing on:

- 1.) Electronic stopping power
- 2.) Density of states
- 3.) Dynamic structure factor

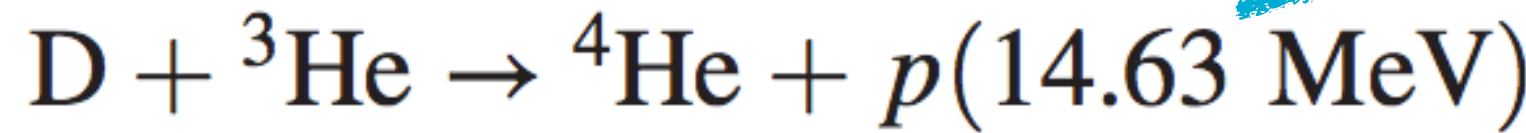
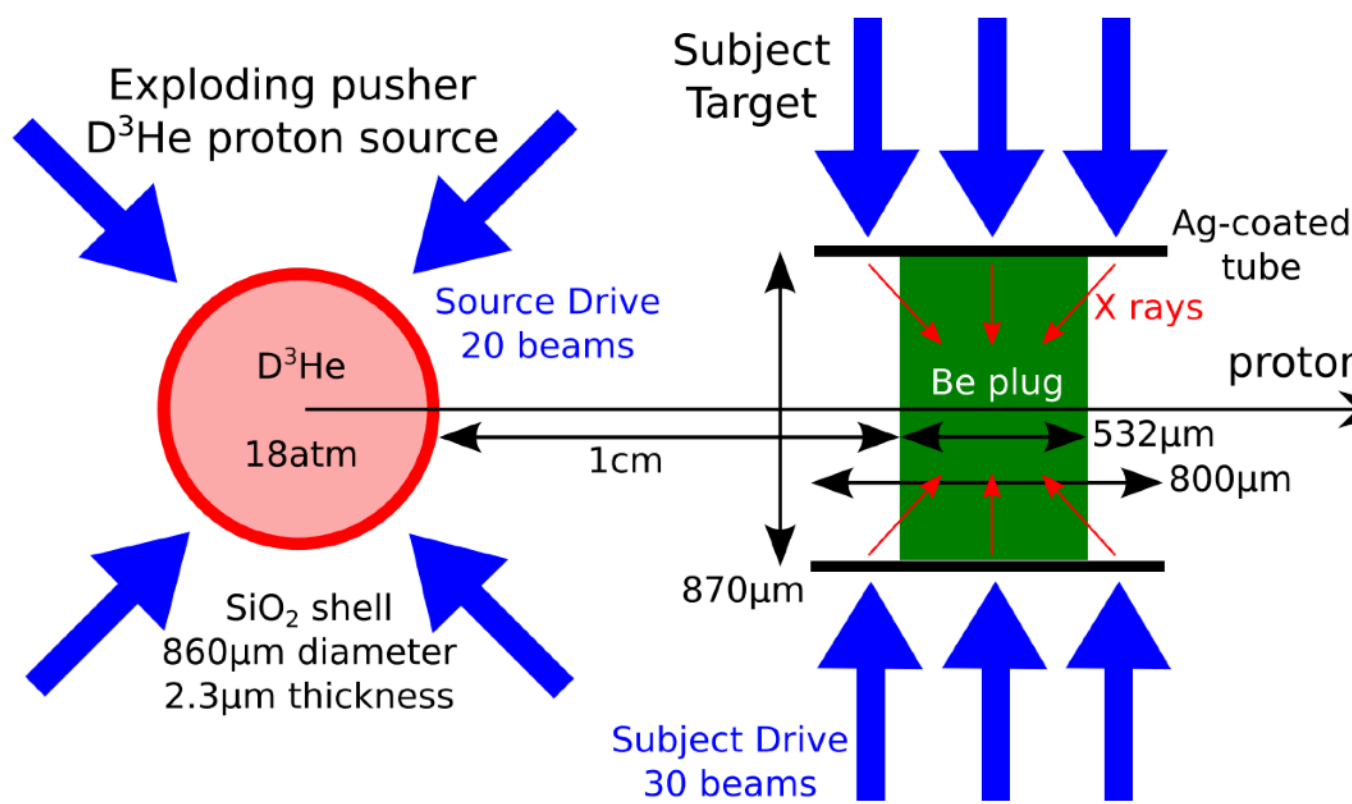
TDDFT isn't a replacement for an experiment, but it still highlights improvements in AA.

*Notably, there are tabular DFT models that take $O(\text{months})$ to develop on $O(10\text{k cores})$, but there are good reasons to do it faster and/or save the CO_2 emissions.

Electronic stopping powers

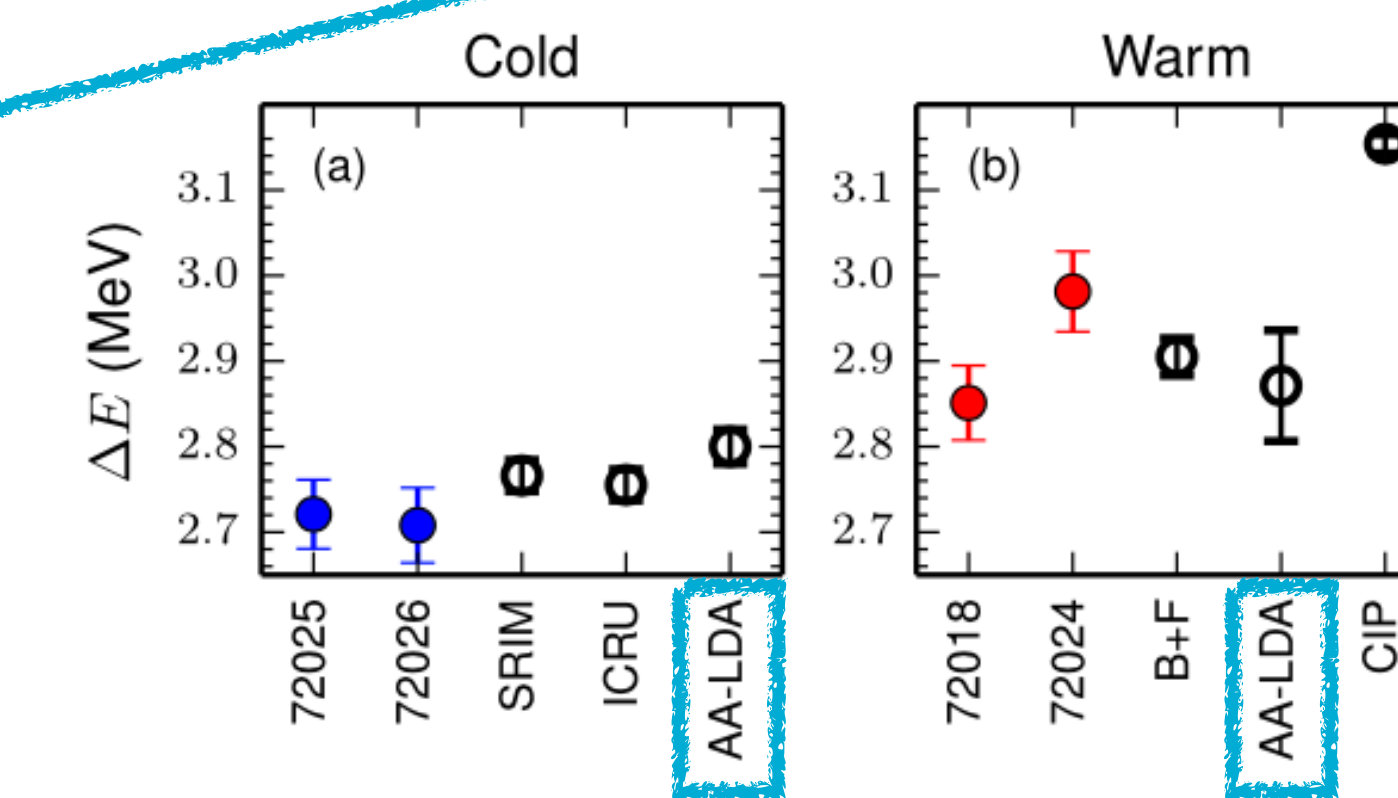
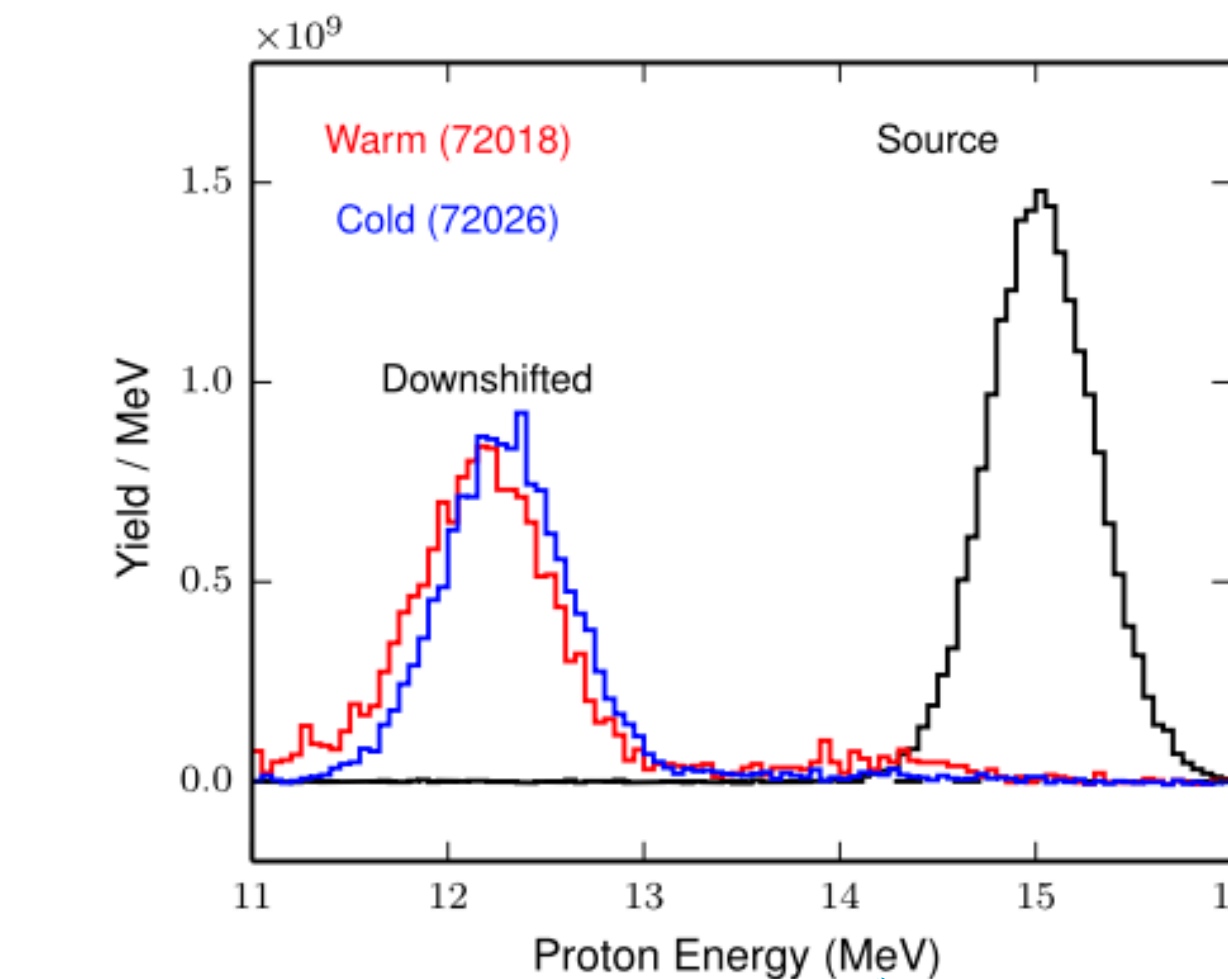
Experimental motivation

Measurement of Charged-Particle Stopping in Warm Dense Plasma
 A. B. Zylstra, J. A. Frenje, P. E. Grabowski, C. K. Li, G. W. Collins, P. Fitzsimmons, S. Glenzer, F. Graziani, S. B. Hansen, S. X. Hu, M. Gatu Johnson, P. Keiter, H. Reynolds, J. R. Rygg, F. H. Séguin, and R. D. Petrasso
 Phys. Rev. Lett. **114**, 215002 – Published 27 May 2015



What is the **energy-dependent force** on a **proton** traversing an **isochorically heated Be plasma** **near 32 eV**?

Stopping at energies relevant to fusion products **dominated by finite size effects**



AA: agrees pretty well w/experiment
 TDDFT: 10 hours on 160,000 CPUs my error bar was bigger than the y-axis

AA approximations in stopping

Results on the previous slide rely on two “big” approximations

- 1.) “Local density approximation” for stopping

Given a formula for the stopping number as a function of density,
average over the density in the calculation.

- 2.) No trajectory dependence

This would be important in a cold solid, but unimportant in a sufficiently hot/disordered system.
But how hot/disordered do we need to be for this to be true?

Subsequent results won’t depend on stopping LDA - instead a dielectric model.

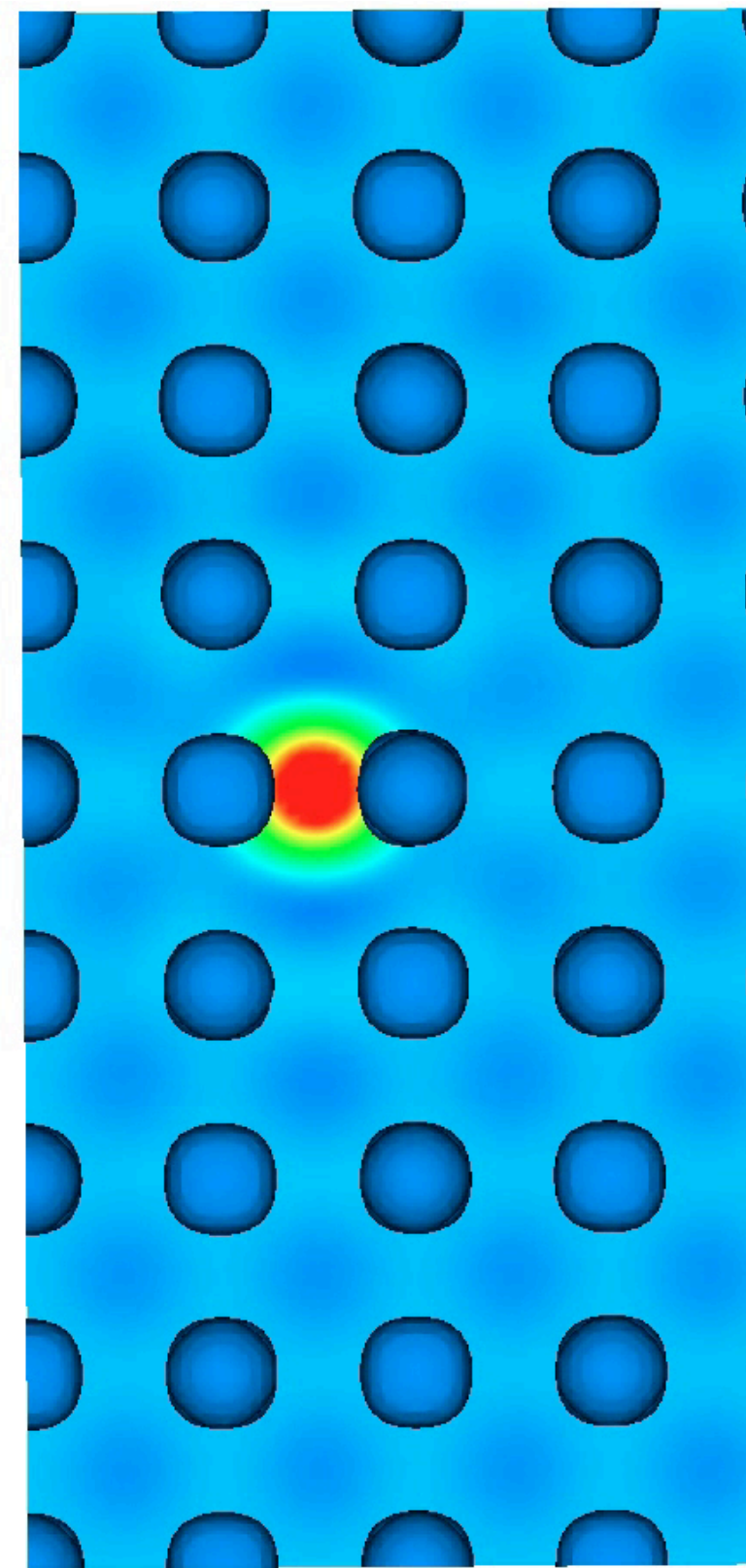
$$S(v) = \frac{2Z_I^2}{\pi v^2} \int_0^\infty \frac{dk}{k} \int_0^{kv} d\omega \omega \text{Im} \left[\frac{-1}{\epsilon(k, \omega)} \right]$$

We’ll use Ehrenfest-TDDFT to assess the sensitivity to trajectories.

(At least) 240,000 words*

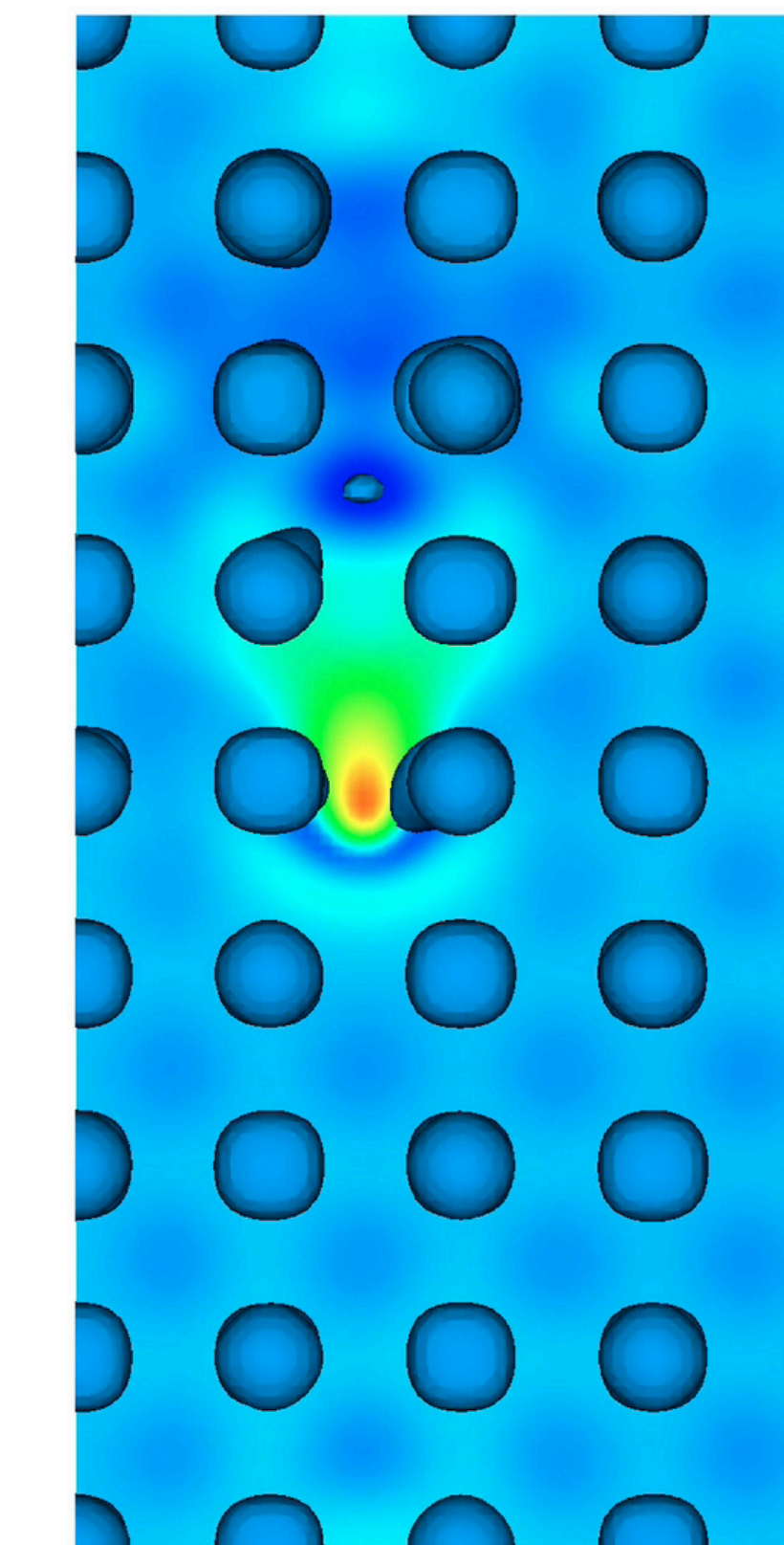
Born-Oppenheimer

Proton velocity



Ehrenfest

Stopping force



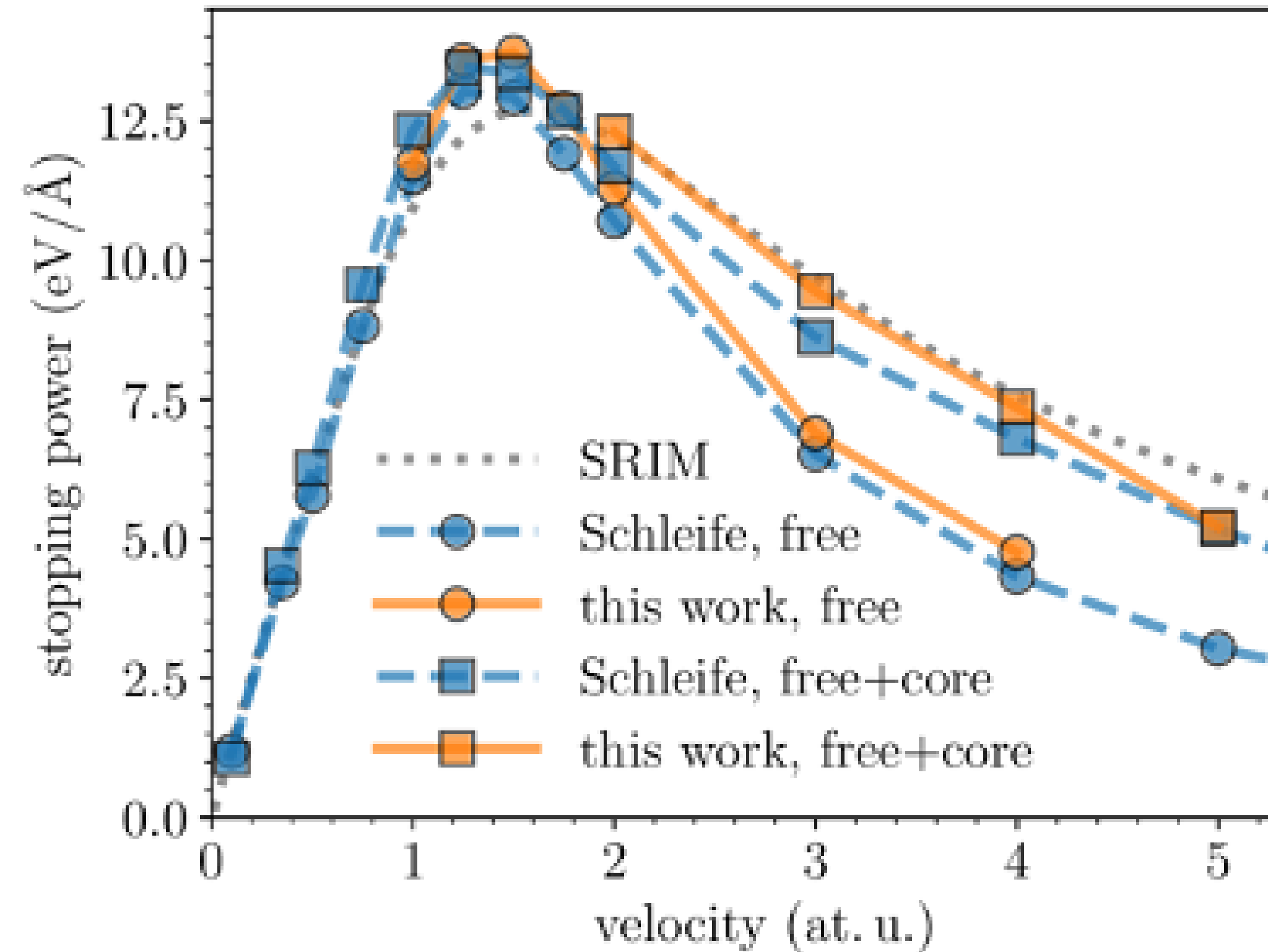
Average force is zero on the left

Average force agrees well with SRIM on the right (see next slide)

*20 pictures per second \times 6 seconds \times 2 movies \times 1,000 words/picture

Quis custodiet ipsos TDDFT?

We've also cross-validated our VASP Ehrenfest-TDDFT implementation against one in QB@II.



These data are for cold fcc aluminum.

QB@II data from:

Schleife, Kanal, and Correa, PRB (2015)

SRIM data from:

Ziegler, Ziegler, & Biersack, Nuc. Inst. & Meth. (2010)

Modest discrepancies are likely due to differences in trajectories and pseudization.

Comparing collisional models in AA

Next, we compare TDDFT and three different collisional models in AA

The system under consideration is “isochorically heated” aluminum @ 1 eV

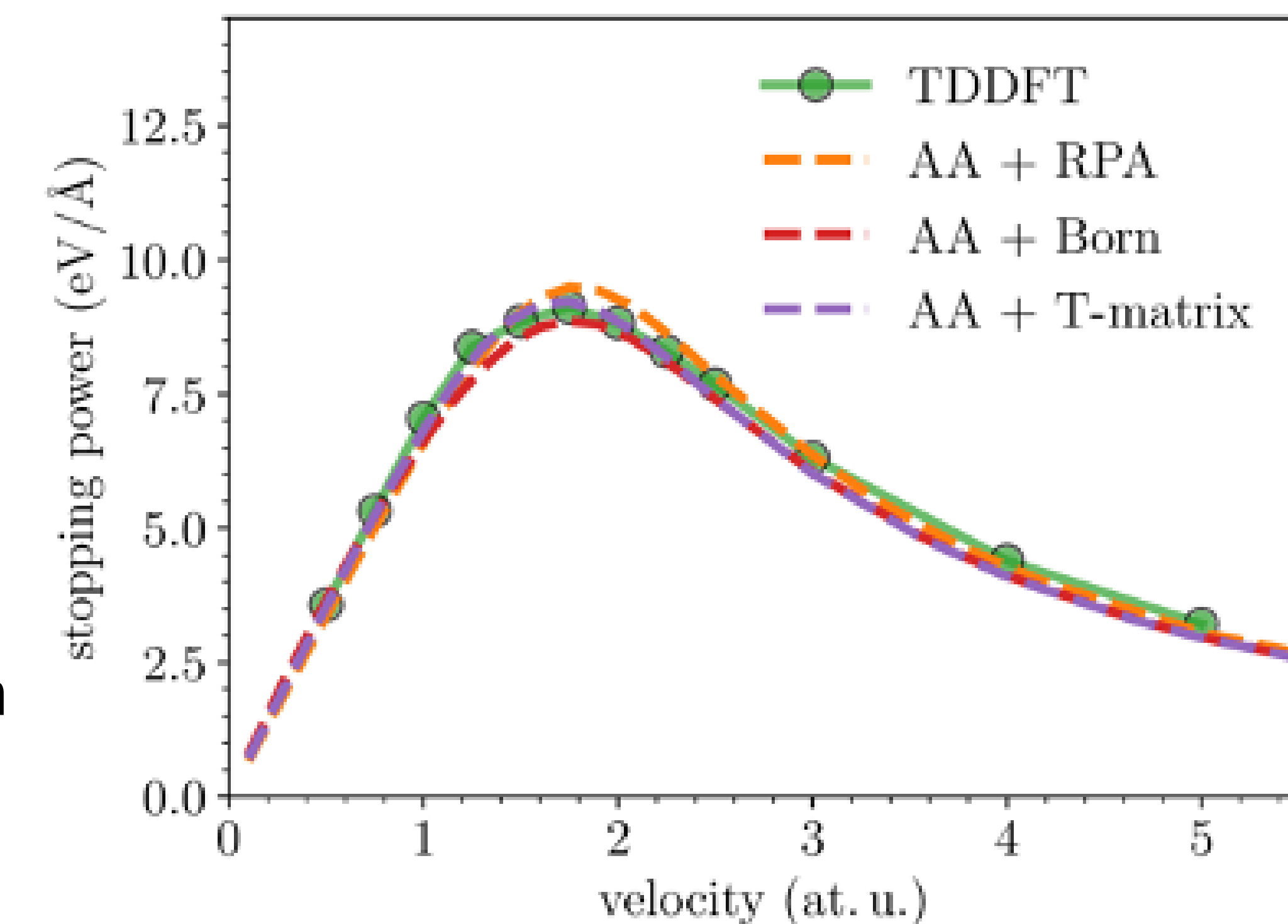
We only consider the “free” electrons, here.

All but 3 electrons/atom are frozen in TDDFT.

$$S(v) = \frac{2Z_I^2}{\pi v^2} \int_0^\infty \frac{dk}{k} \int_0^{kv} d\omega \omega \text{Im} \left[\frac{-1}{\epsilon(k, \omega)} \right]$$

Stopping powers generally agree pretty well, though we will later see clear differences between RPA and T-matrix approaches in the DSF.

What about trajectory dependence?



Hentschel, et al., in preparation (2022)

Quantifying “typical” trajectories

Local environment of projectile characterizes trajectory:
specifically **distribution of nearest neighbor (NN) distances**

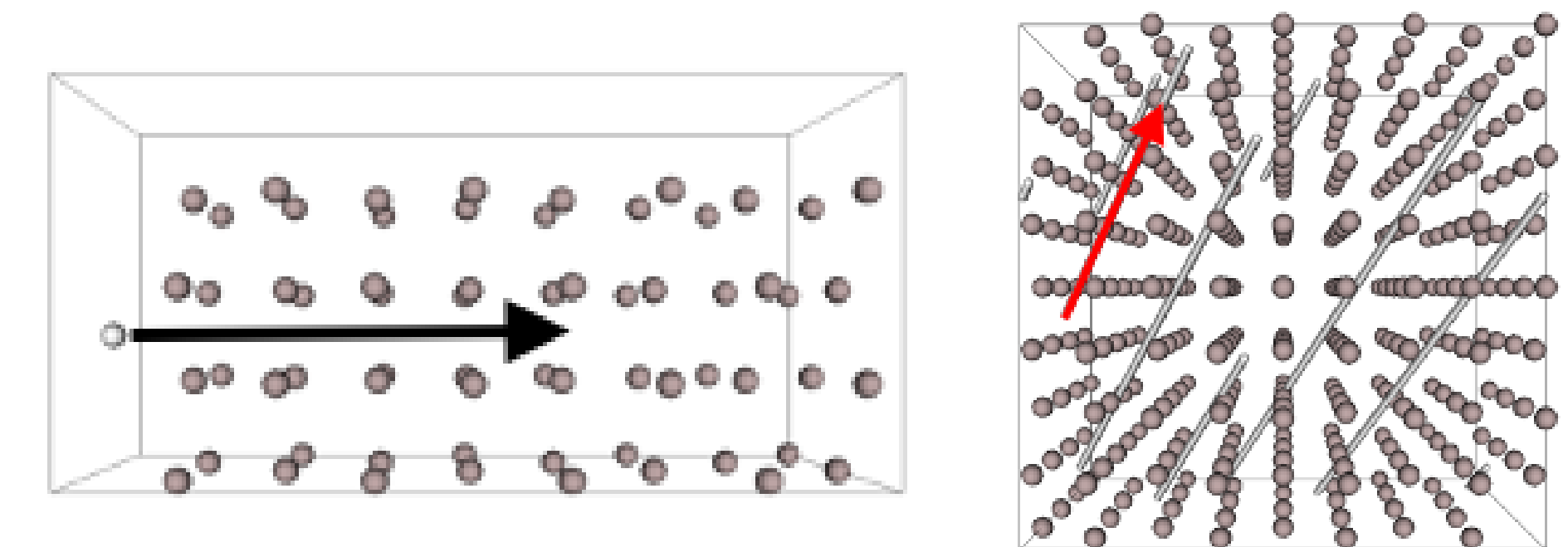
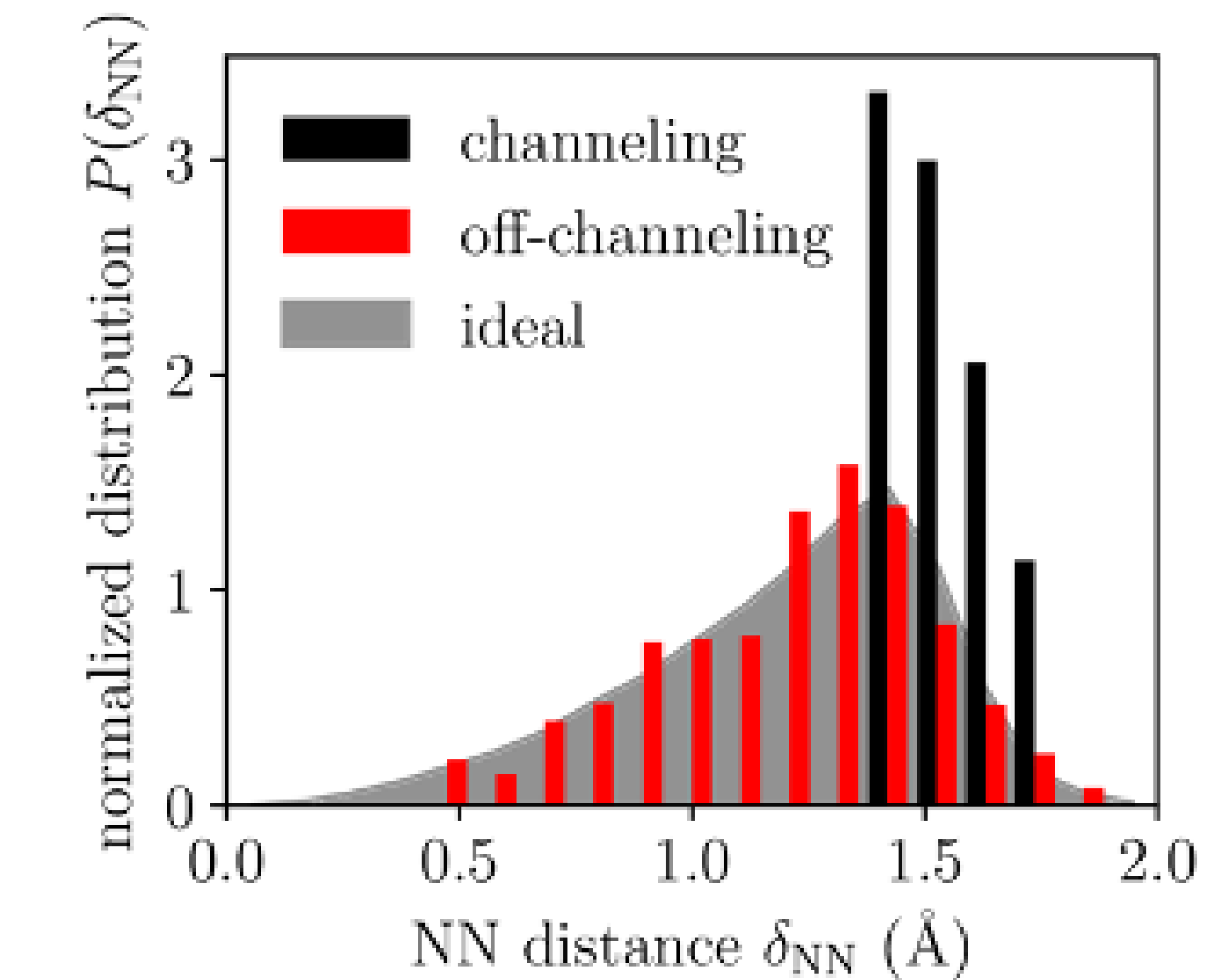
Ideal NN distribution: uniform random sampling of cell

Bhattacharyya distance quantifies the distance between
two distributions

$$D_B = -\ln \left(\int d\delta_{NN} \sqrt{P_{traj}(\delta_{NN})P_{ideal}(\delta_{NN})} \right)$$

Typical trajectories will have smaller Bhattacharyya distances

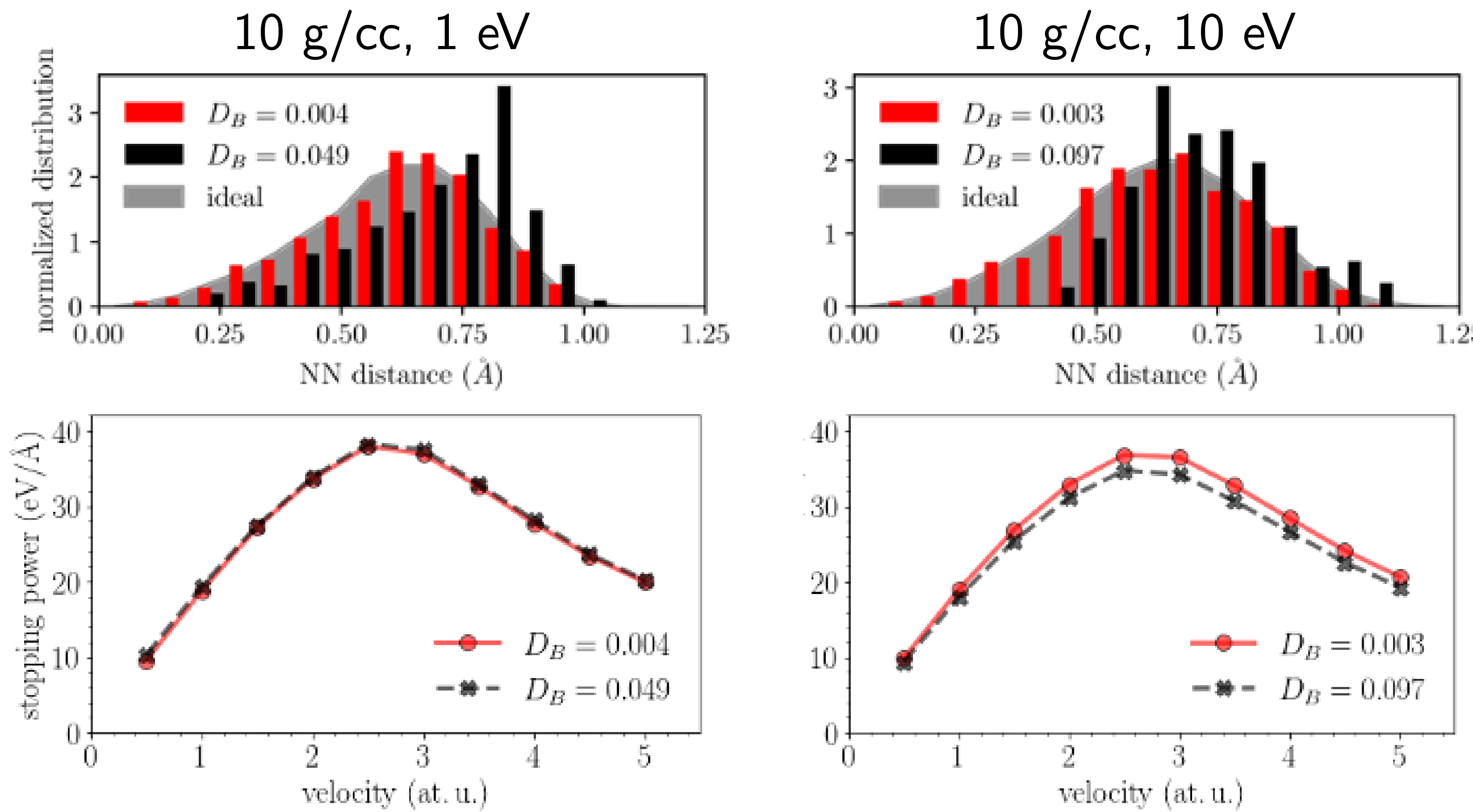
Note that the off-channeling trajectory gave us good
agreement with SRIM.



Trajectory-dependence of stopping

For warm dense carbon, it is hard to find a “bad” trajectory.

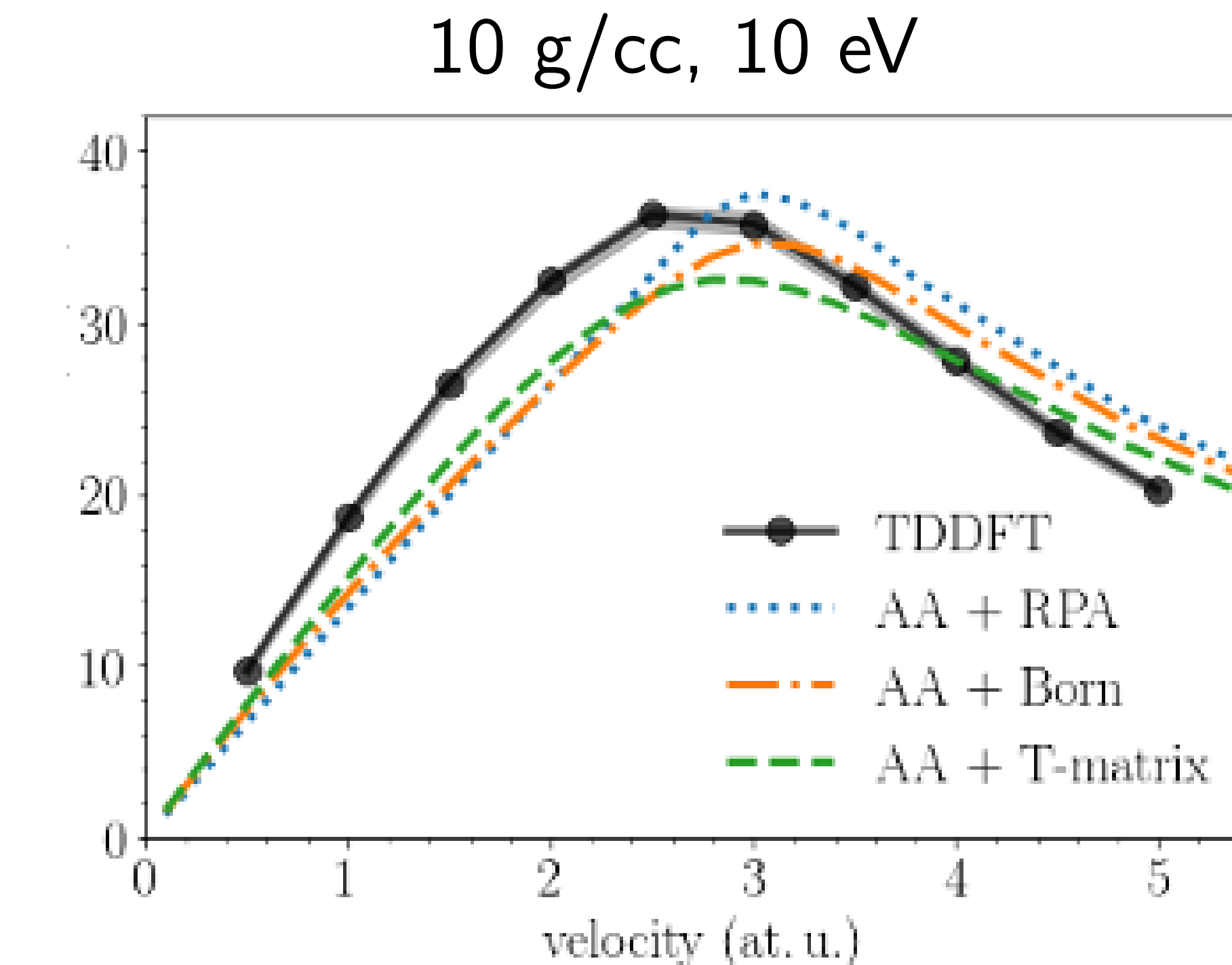
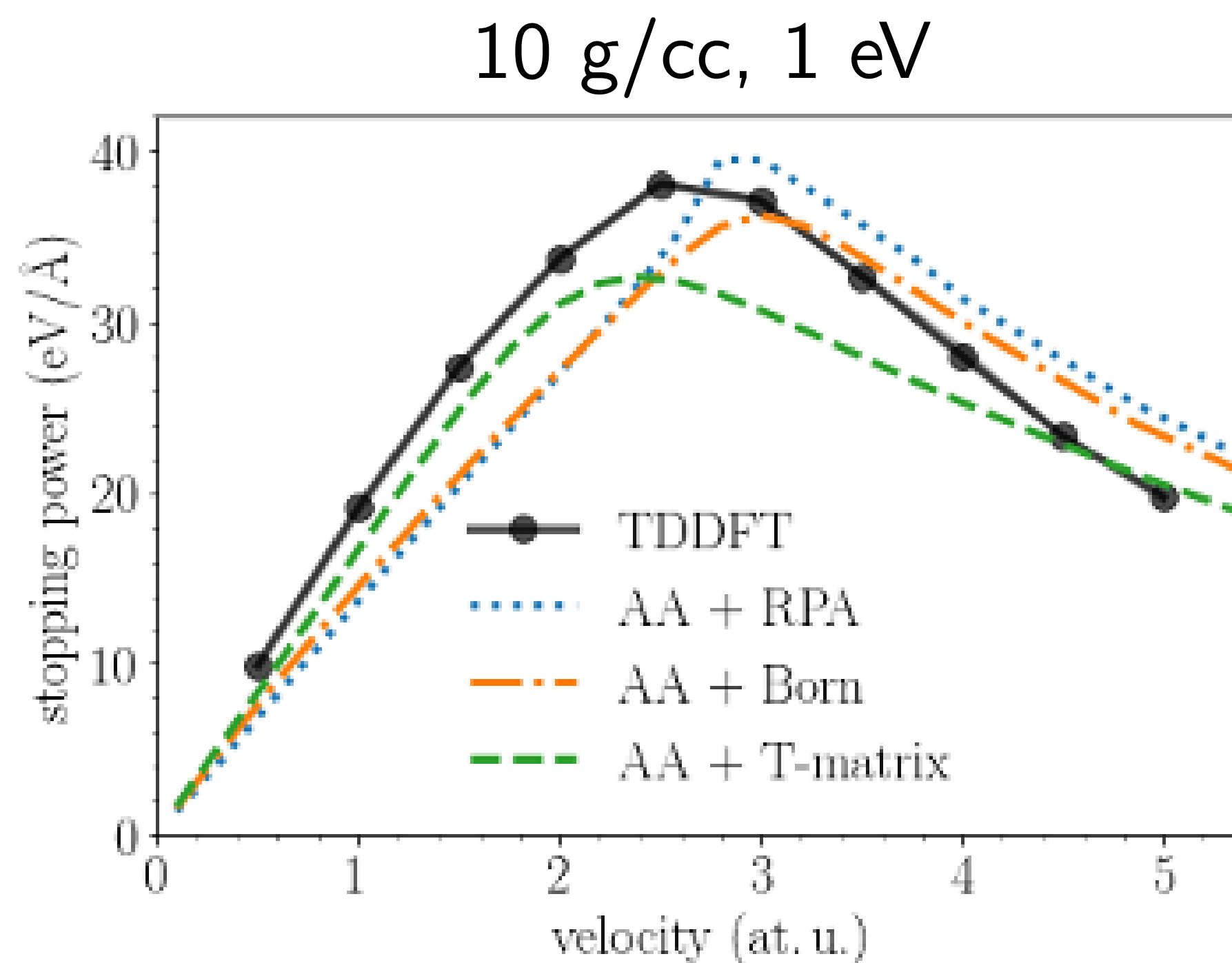
Little sensitivity to proton trajectory (below) or snapshot - **good for AA in these conditions!**



Back to collisional models

Discrepancy b/w AA and TDDFT likely due to collisional models in the former
RPA and Born predict a more accurate Bragg peak height
T-matrix predicts more accurate Bragg peak position, low-v slope

But the AA models could still stand to be improved



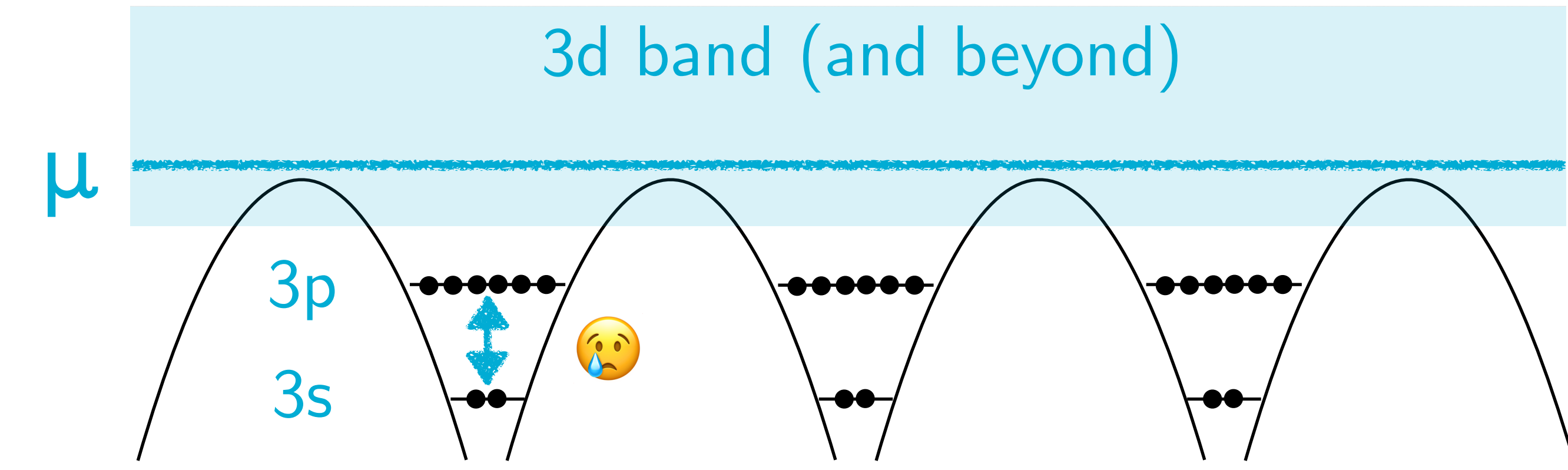
Densities of states and dynamic structure factors

Bound-bound transitions in warm dense matter

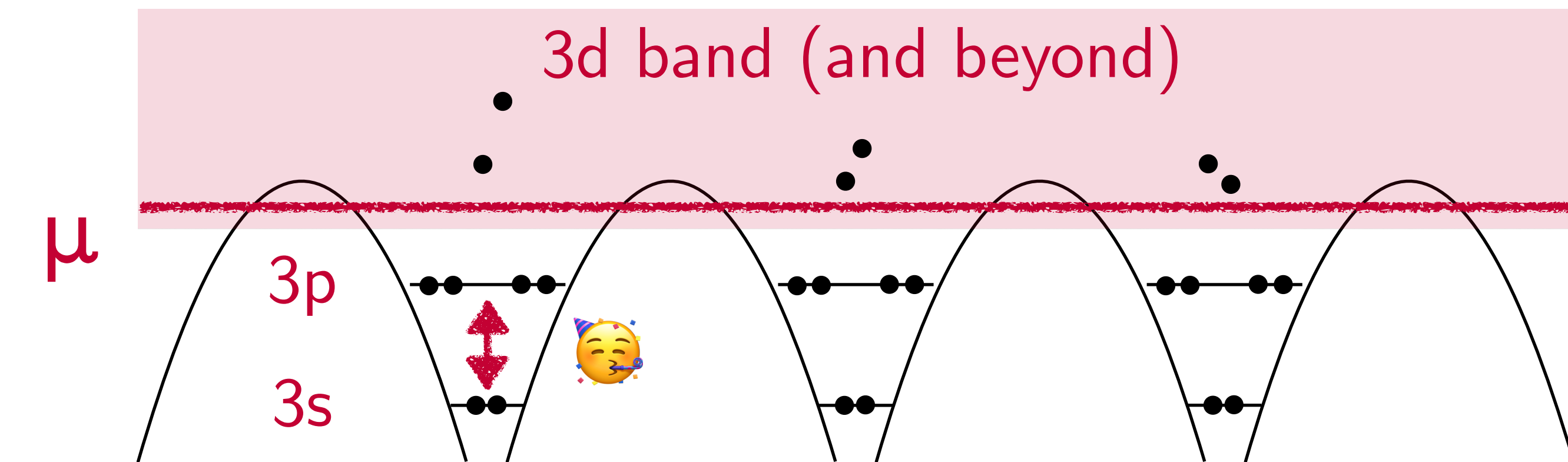
The bulk properties of degenerate matter are defined by the **Pauli exclusion principle**.

Exactly one electron is allowed to have the quantum numbers that it has...

Thermal excitation means that certain electronic rearrangements that would be forbidden are now allowed...



Solid density iron (8 g/cc)



Today, I'll show you how we're modeling these processes as they should appear in scattering experiments, using **time-dependent DFT** and **average atom**.

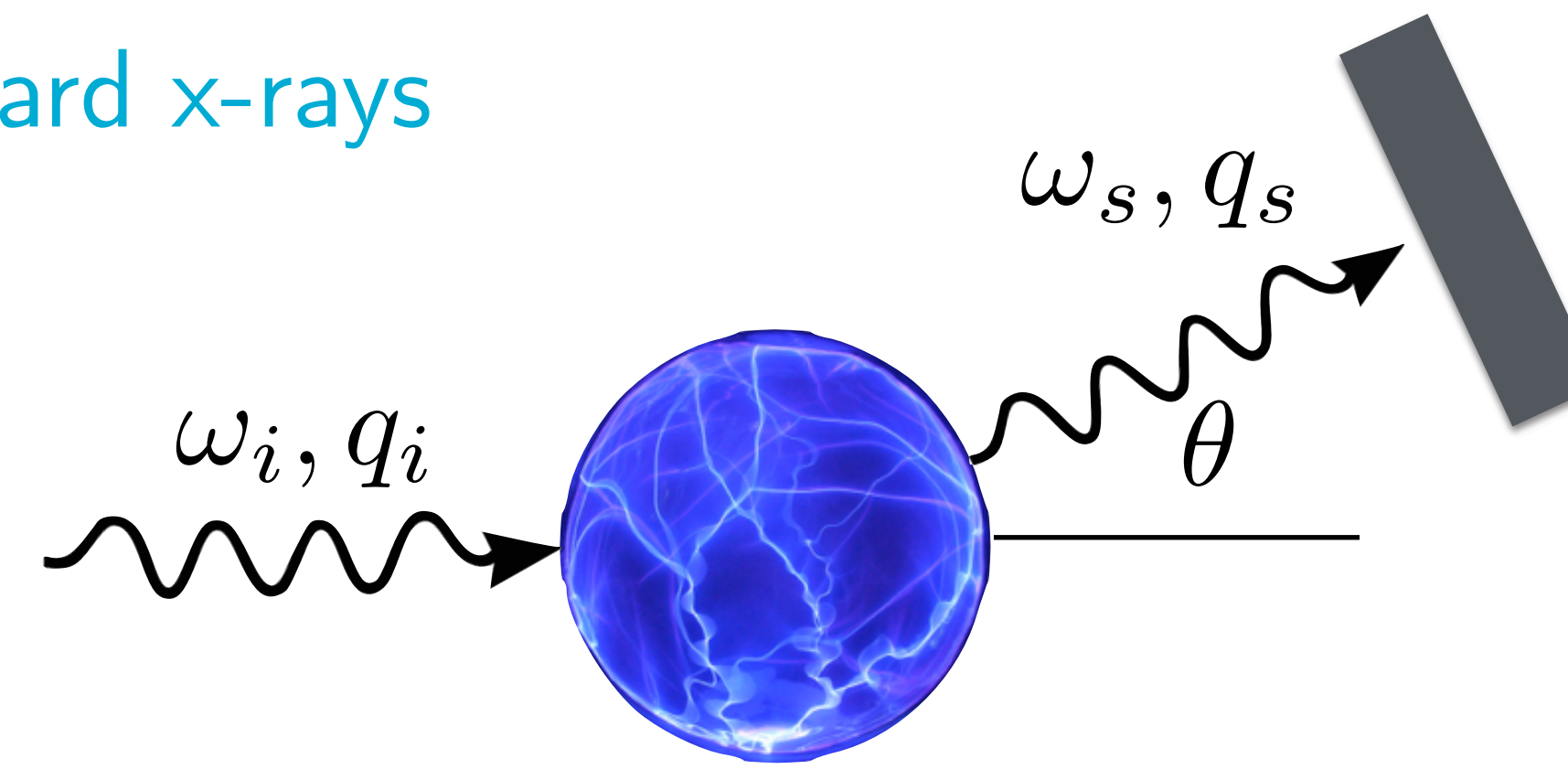
Basics of x-ray Thomson scattering (XRTS)

X-ray Thomson scattering in high energy density plasmas

Siegfried H. Glenzer and Ronald Redmer
Rev. Mod. Phys. **81**, 1625 – Published 1 December 2009

Measure inelastically scattered x-rays

Penetrate with hard x-rays



$$\omega = \omega_i - \omega_s$$
$$q = q_i - q_s$$

$$q = 2q_i \sin(\theta/2)$$

Sample of WDM
(opaque to optical probes)

$$\frac{d^2\sigma}{d\Omega d\omega} = \sigma_T \frac{q_s}{q_i} S(q, \omega)$$

Cross section proportional to dynamic structure factor (DSF)

Contains information about density, ionization state, structure, temperature, etc...

Dynamic structure factor in TDDFT

X-ray Thomson Scattering in Warm Dense Matter without the Chihara Decomposition

A. D. Baczevski, L. Shulenburger, M. P. Desjarlais, S. B. Hansen, and R. J. Magyar
Phys. Rev. Lett. **116**, 115004 – Published 18 March 2016

Probe system with x-ray*

$$v_{pert}(\mathbf{r}, t) = v_0 e^{i\mathbf{q} \cdot \mathbf{r}} f(t)$$

Record density response

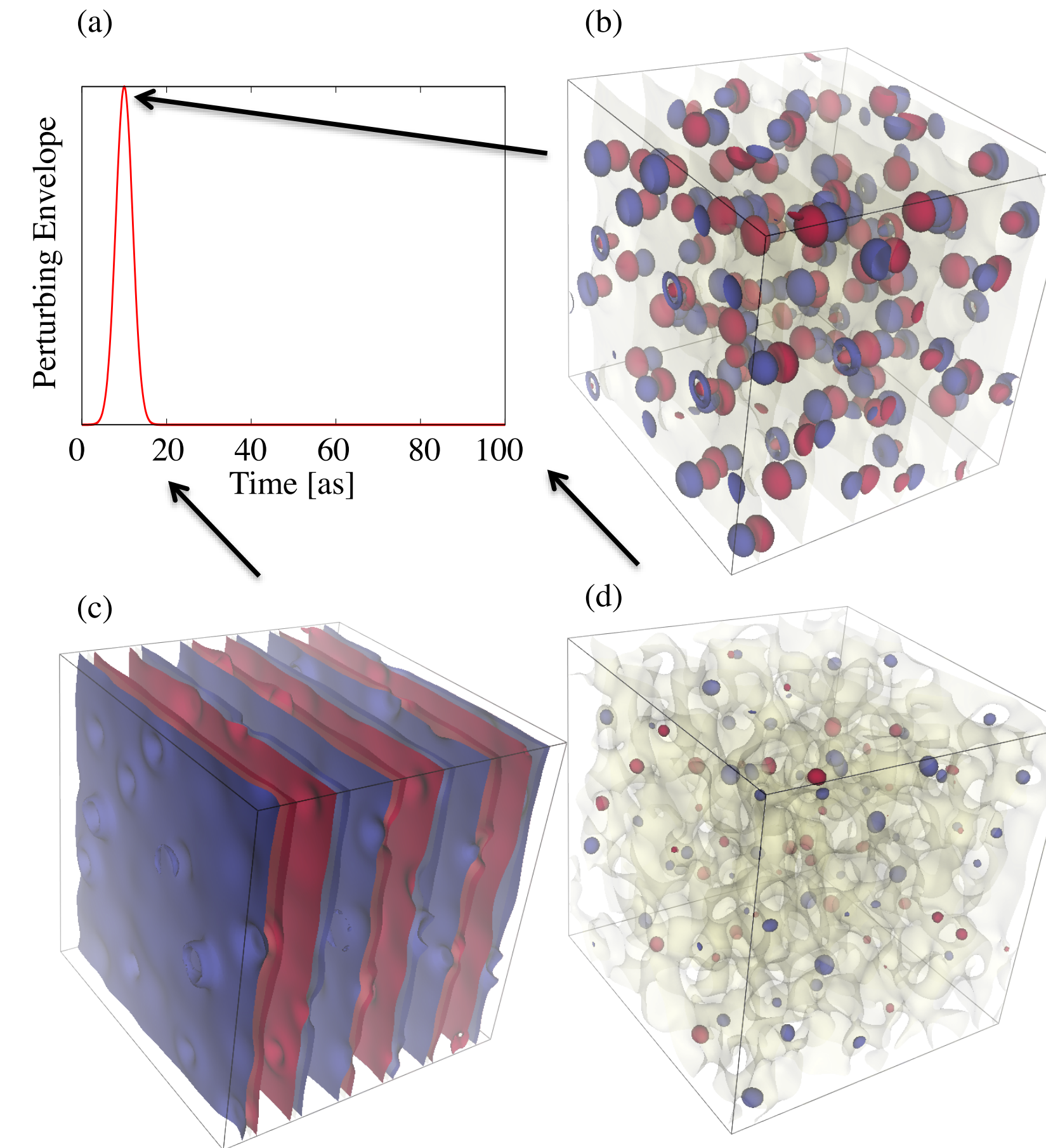
$$\delta\rho(\mathbf{q}, t) = \int_0^\infty d\tau \chi_{\rho\rho}(\mathbf{q}, -\mathbf{q}, \tau) v_0 f(t - \tau)$$

Apply fluctuation-dissipation

$$\chi_{\rho\rho}(\mathbf{q}, -\mathbf{q}, \omega) = \frac{\delta\rho(\mathbf{q}, \omega)}{v_0 f(\omega)}$$

$$S(\mathbf{q}, \omega) = -\frac{1}{\pi} \frac{\text{Im} [\chi_{\rho\rho}(\mathbf{q}, -\mathbf{q}, \omega)]}{1 - e^{-\omega/k_B T_e}}$$

*energy/wave vector set by energy/momentum transfer of interest



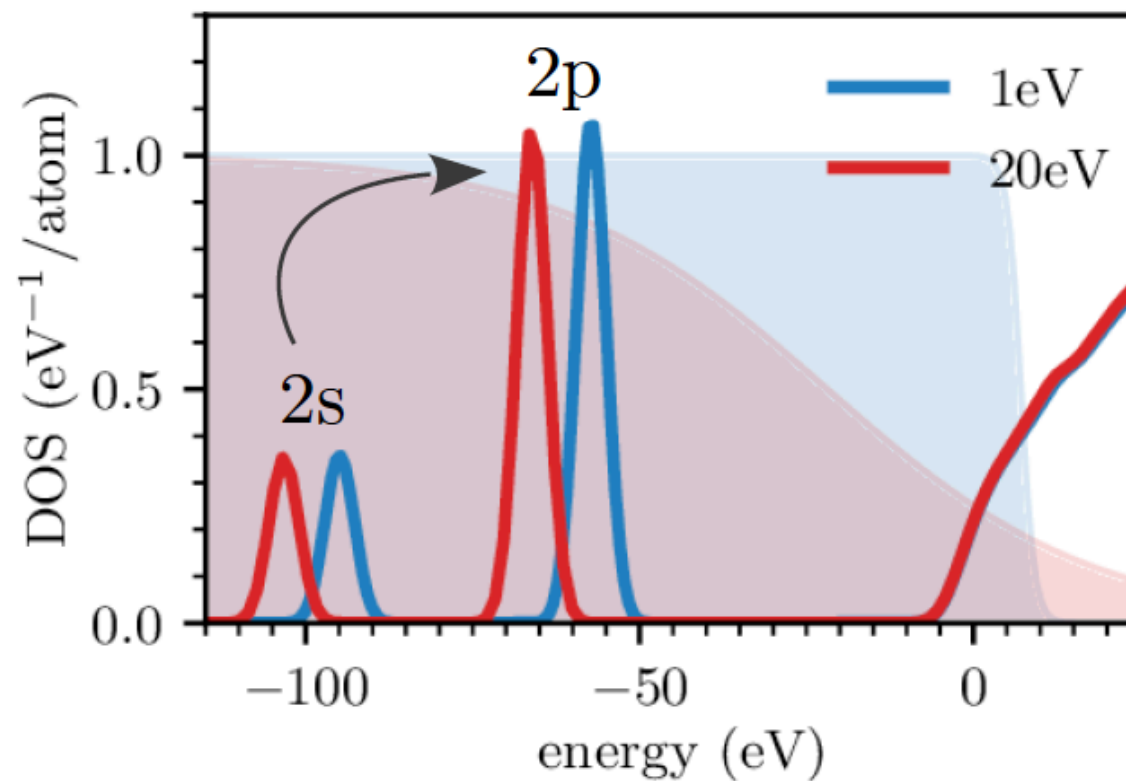
Revising average atom theory

We make 3 significant revisions to work in
[Starrett + Saumon, HEDP, 2014] and [Souza, et al., PRE, 2014]

1. An improved treatment of electron-ion collisions.
Vastly improves the treatment of the plasmon, in general.
2. The addition of a bound-bound term to the Chihara decomposition.
Think of this as a label for matrix elements for Kramers-Heisenberg.
3. Use of the non-ideal density of states.
Obviates the need for separate treatment of quasi-bound states.

Example 1: Aluminum (“good” free-electron metal)

Thermal depletion of 2p states starts to appear above 10 eV
[Witte, et al., PoP, 2018]

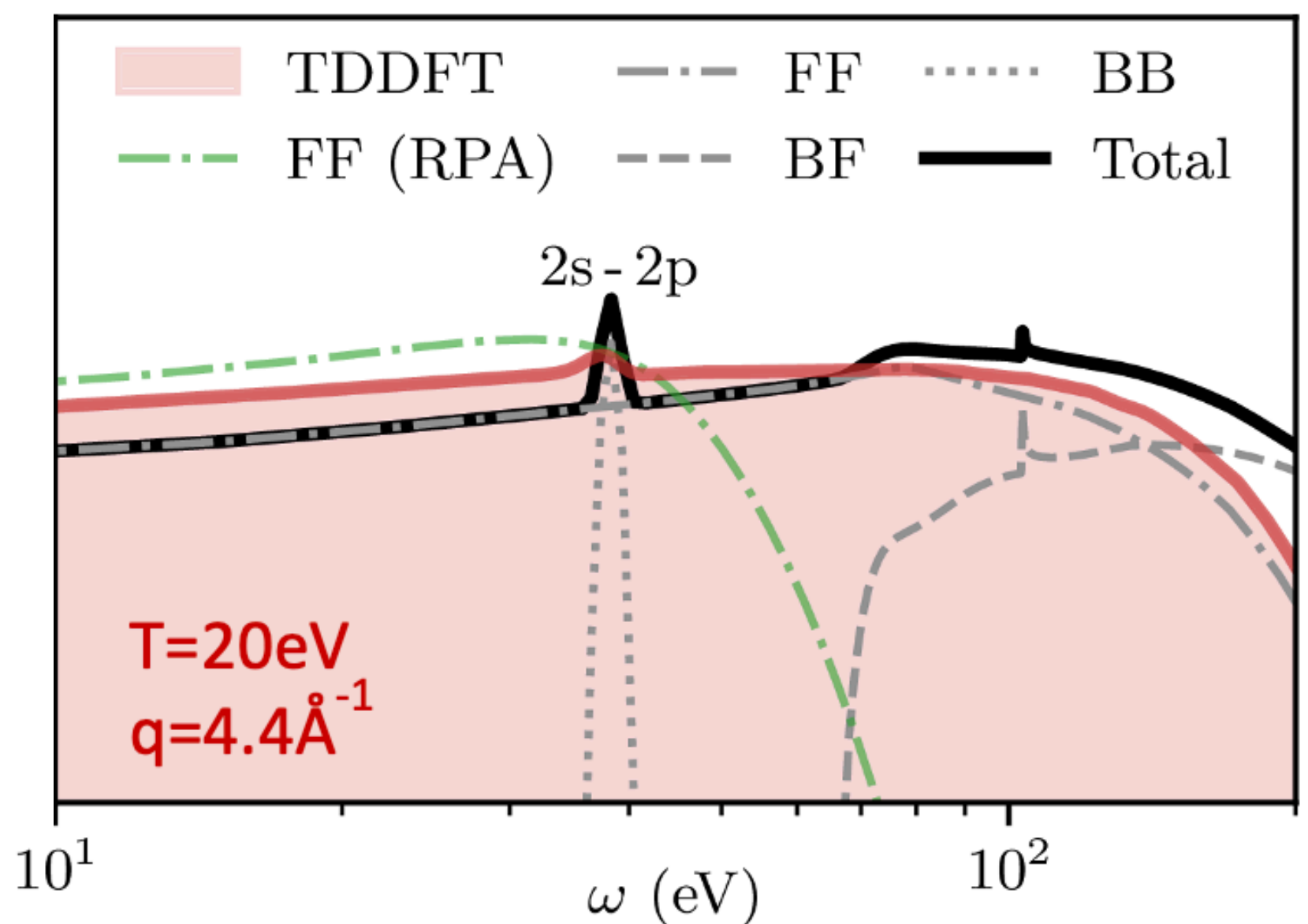
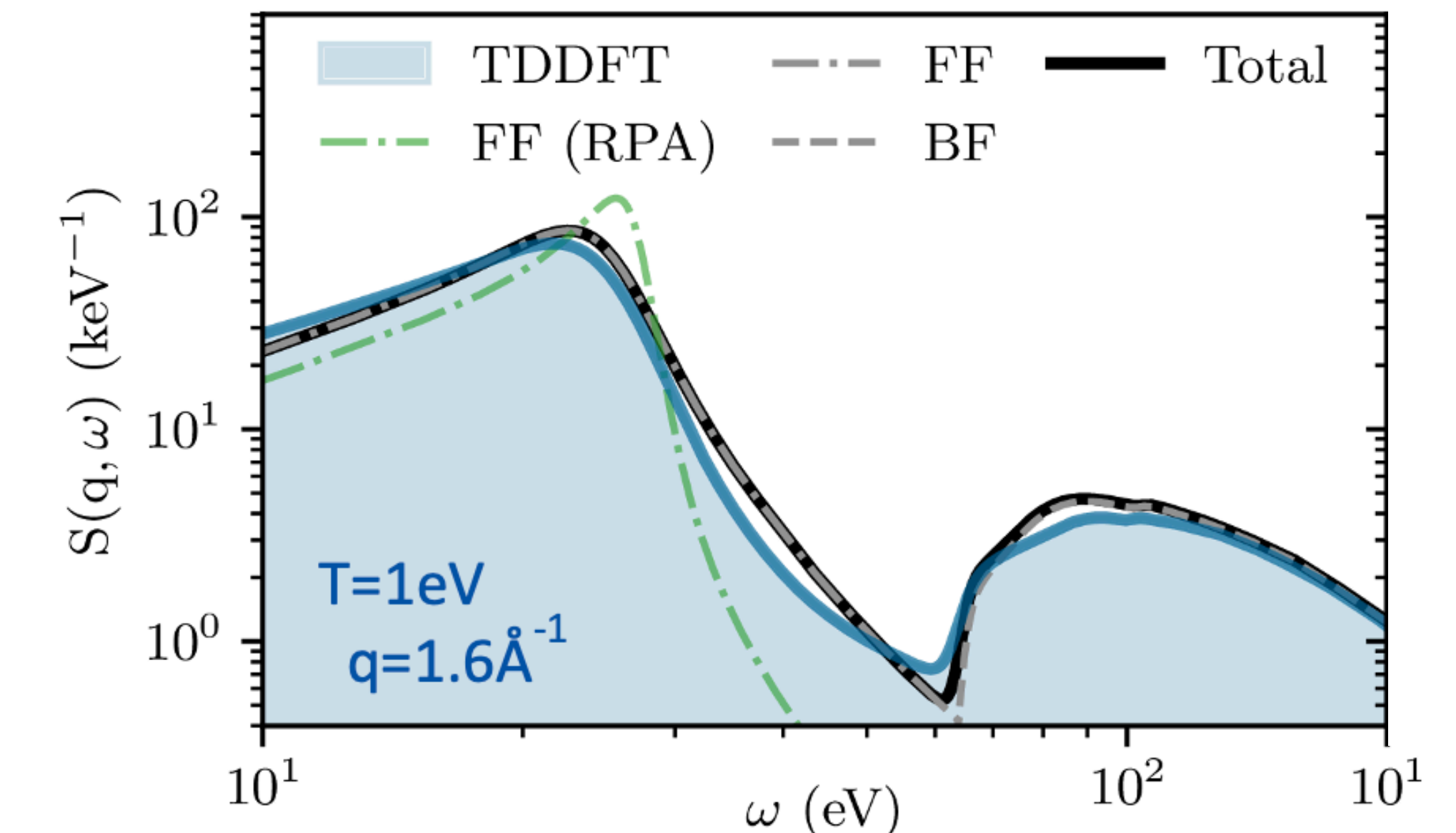


Results highlight the importance of revised Mermin treatment of the free-free contribution over RPA.

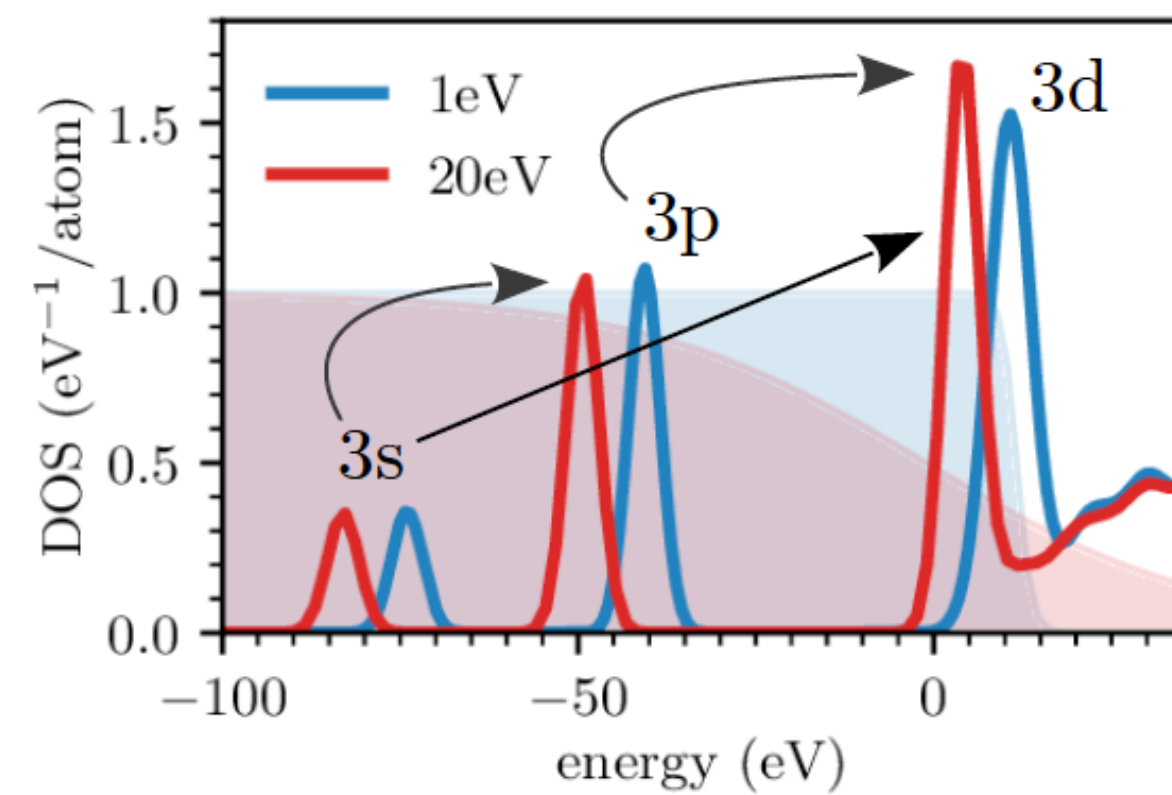
A 2s-2p bound-bound transition appears coincident with thermal depletion of 2p.

Low intensity, but if you see such a feature you have a smoking gun that you're above ~ 10 eV.

Key takeaway: bound-bound might be weak, but this example illustrates need for better collisions in AA.



Example 2: Iron (d-band near chemical potential)



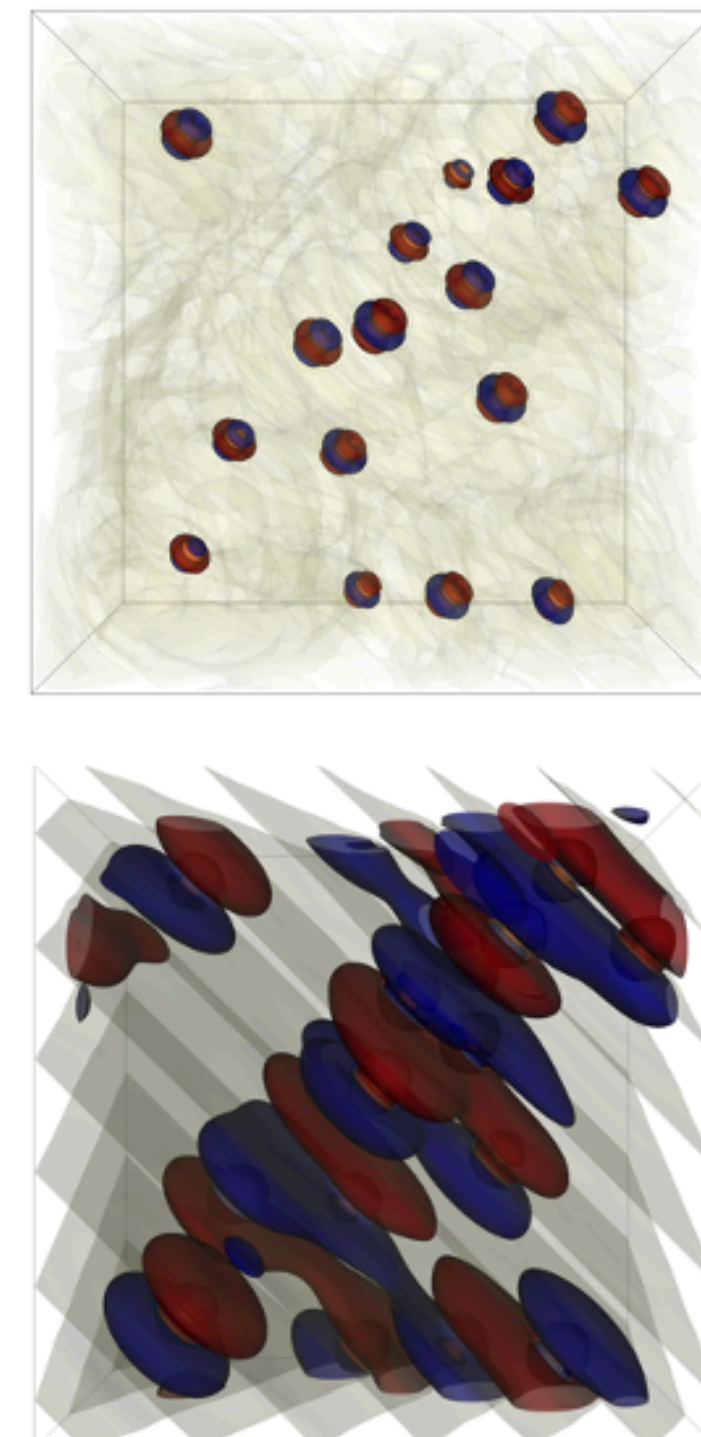
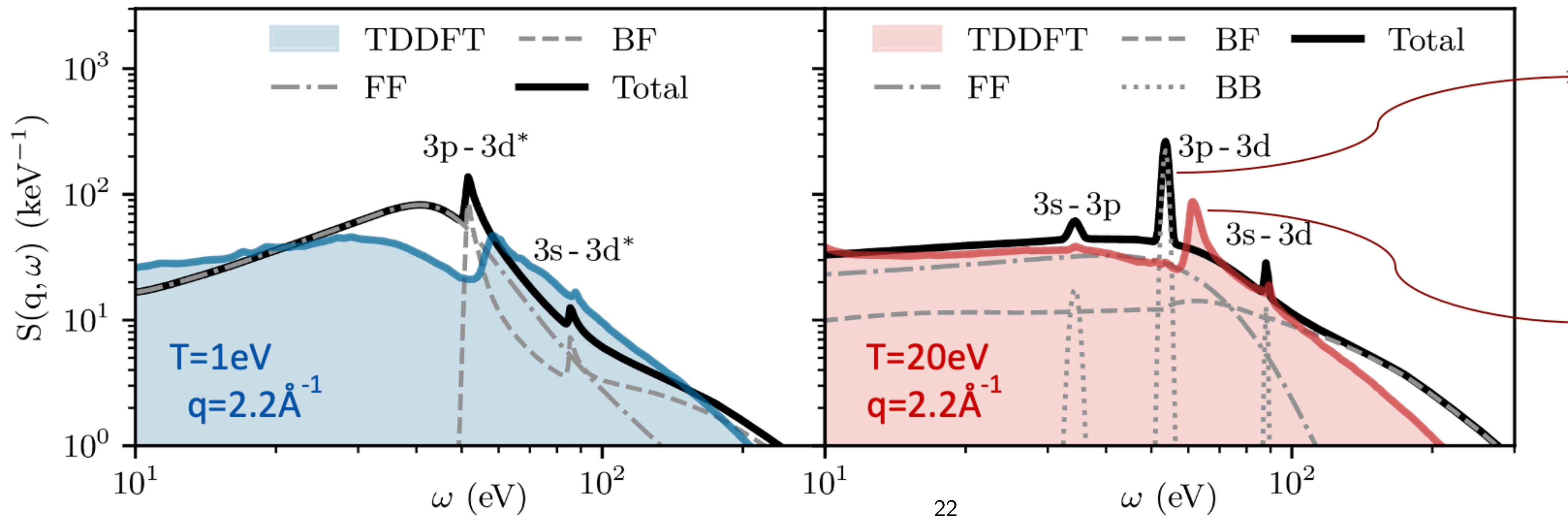
The spectrum of bound-bound transitions is richer yet in iron.

$3p \rightarrow 3d$ @ 55 eV

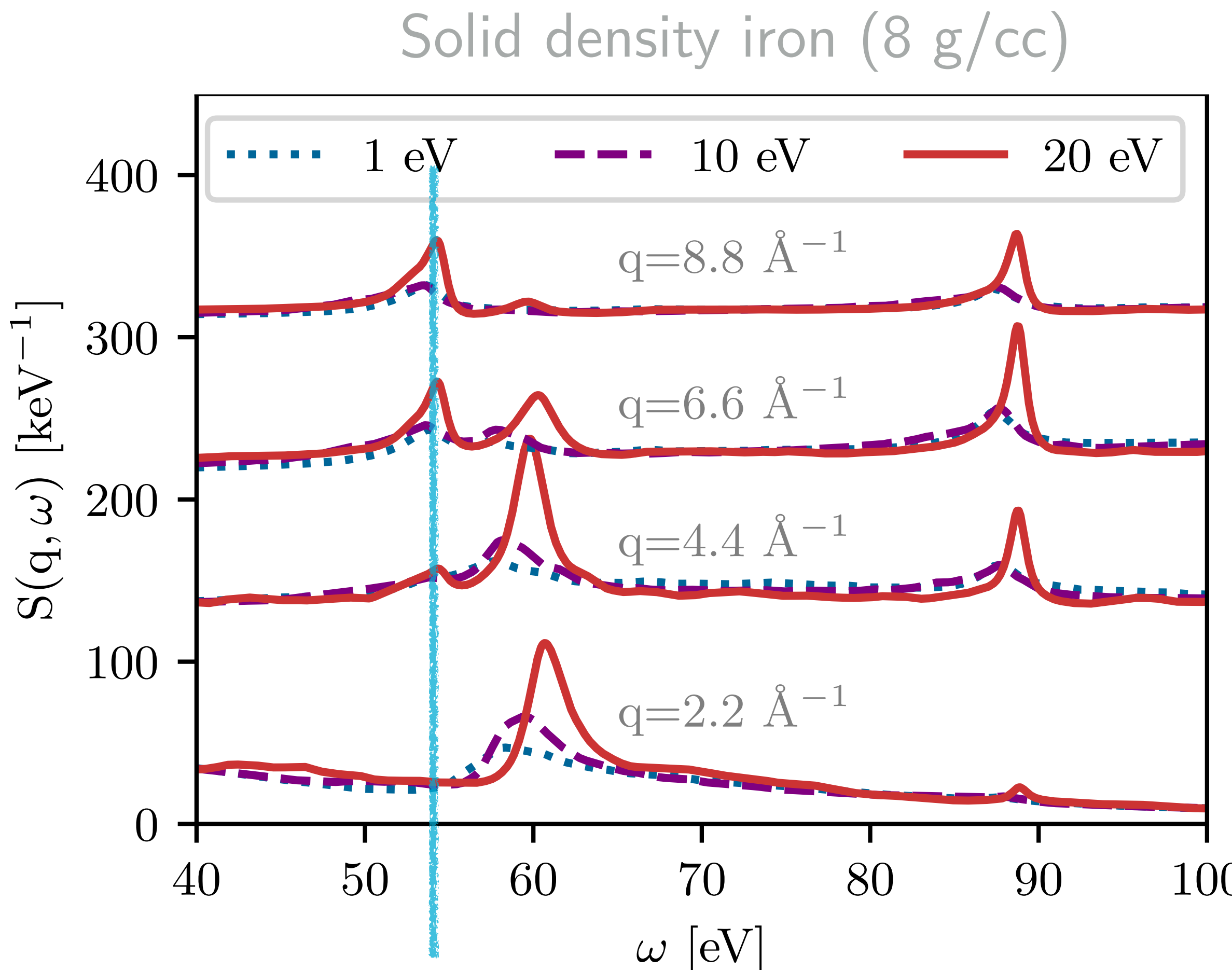
$3s \rightarrow 3d$ @ 85 eV

$3s \rightarrow 3p$ @ 35 eV

There is a ~ 5 eV discrepancy between TDDFT and average atom for 3p-3d, worth further consideration...



Collective character of the iron 3p-3d feature



Average atom predicts a non-dispersing bound-bound feature at 54 eV.

TDDFT predicts that a **single-particle excitation** around 54 eV will appear at large momentum transfers...

...but at smaller momentum transfers, this excitation has a **collective character** that gets stronger with temperature.

We have confirmed:

- 1) Not an exchange-correlation effect,
- 2) Kubo-Greenwood fails to reproduce.

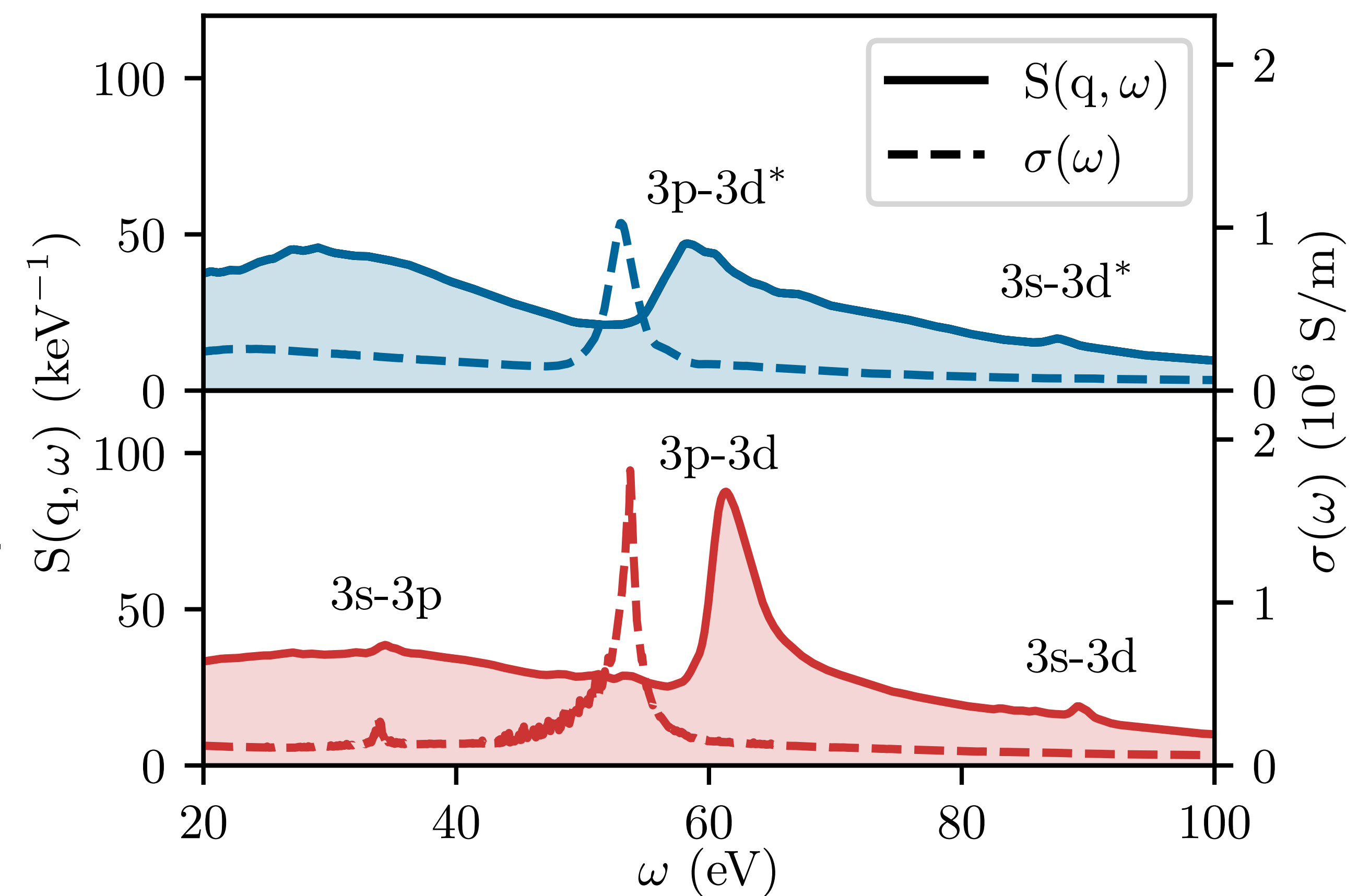
3d isn't *really* a bound state, it is a narrow band near the chemical potential.

Failure of Kubo-Greenwood*

Treatment of the Kubo-Greenwood* dielectric function common in our community is equivalent to a TDDFT calculation in which the Hartree+exchange-correlation kernel is zero.

Discrepancies between these treatments of the response function are thus entirely due to the neglect of collective effects in Kubo-Greenwood*.

Another way of putting this:
Kubo-Greenwood* is *only* capable of capturing single-particle (non-collective) excitations.



*Important semantic distinction: I'm referring the evaluation of the Kubo-Greenwood formula w/Kohn-Sham orbitals.
If you evaluated the Kubo-Greenwood formula with the exact wave function, this deficiency would not apply.

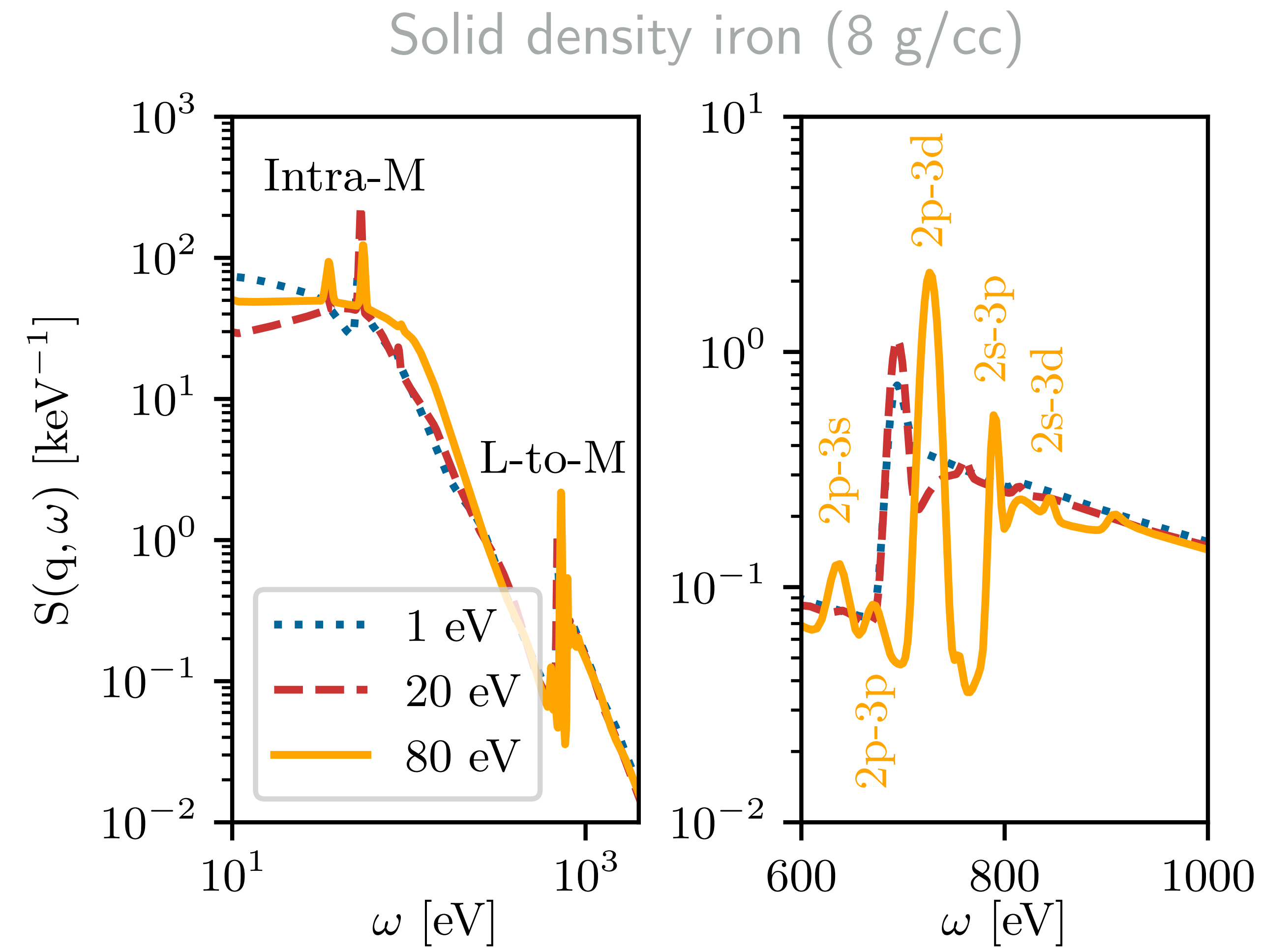
Inter-shell bound-bound processes in average atom

One benefit of average atom is being able to efficiently study conditions that are **prohibitively expensive for TDDFT...**

Looking at the L-shell in TDDFT would require (at least) **$O(100)\times$ the CPU time!**

We see that a rich set of **inter-shell features** around the L-edge at higher temperatures.

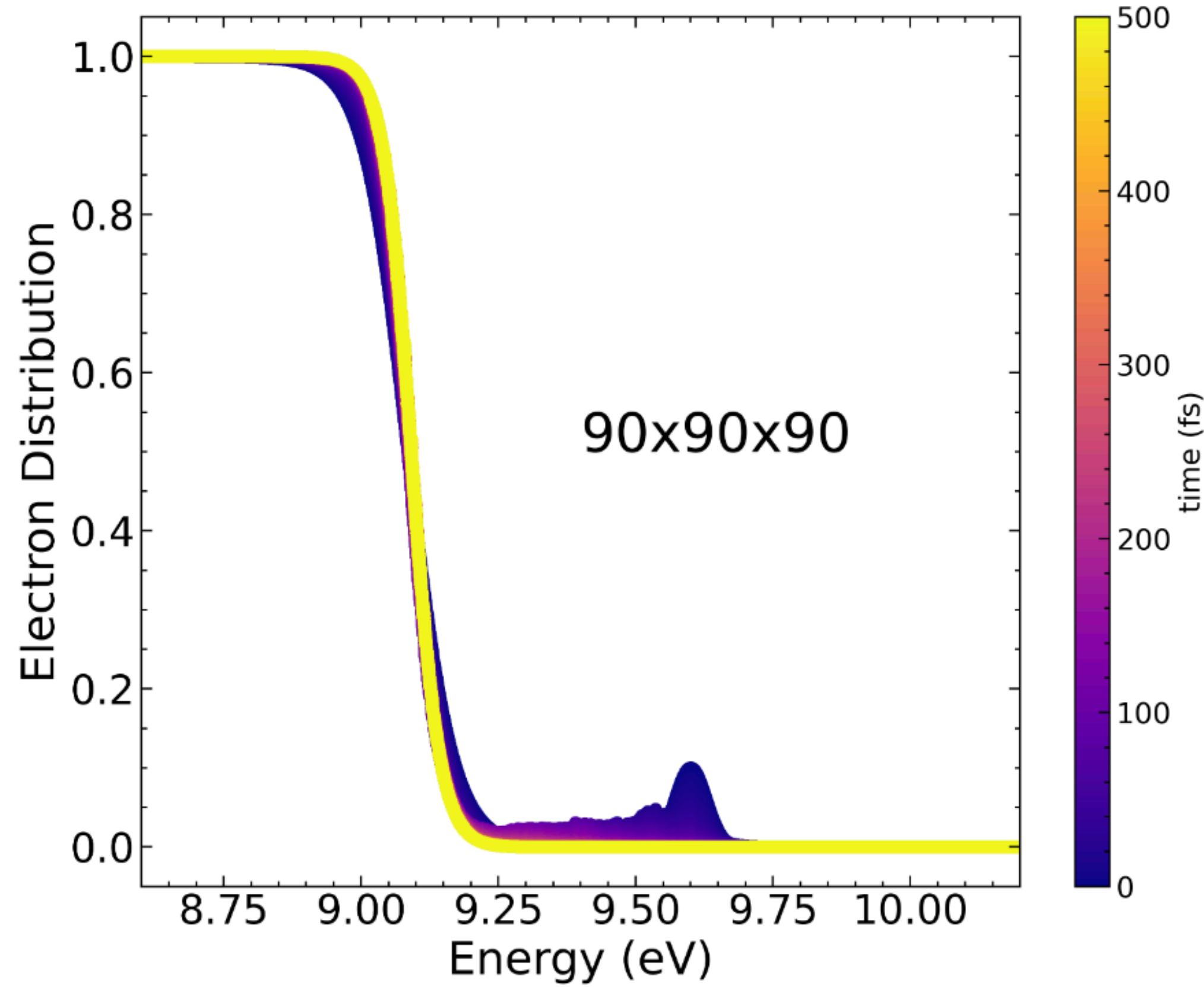
All of these features can be used in thermometry, **better than plasmon shift for certain conditions.**



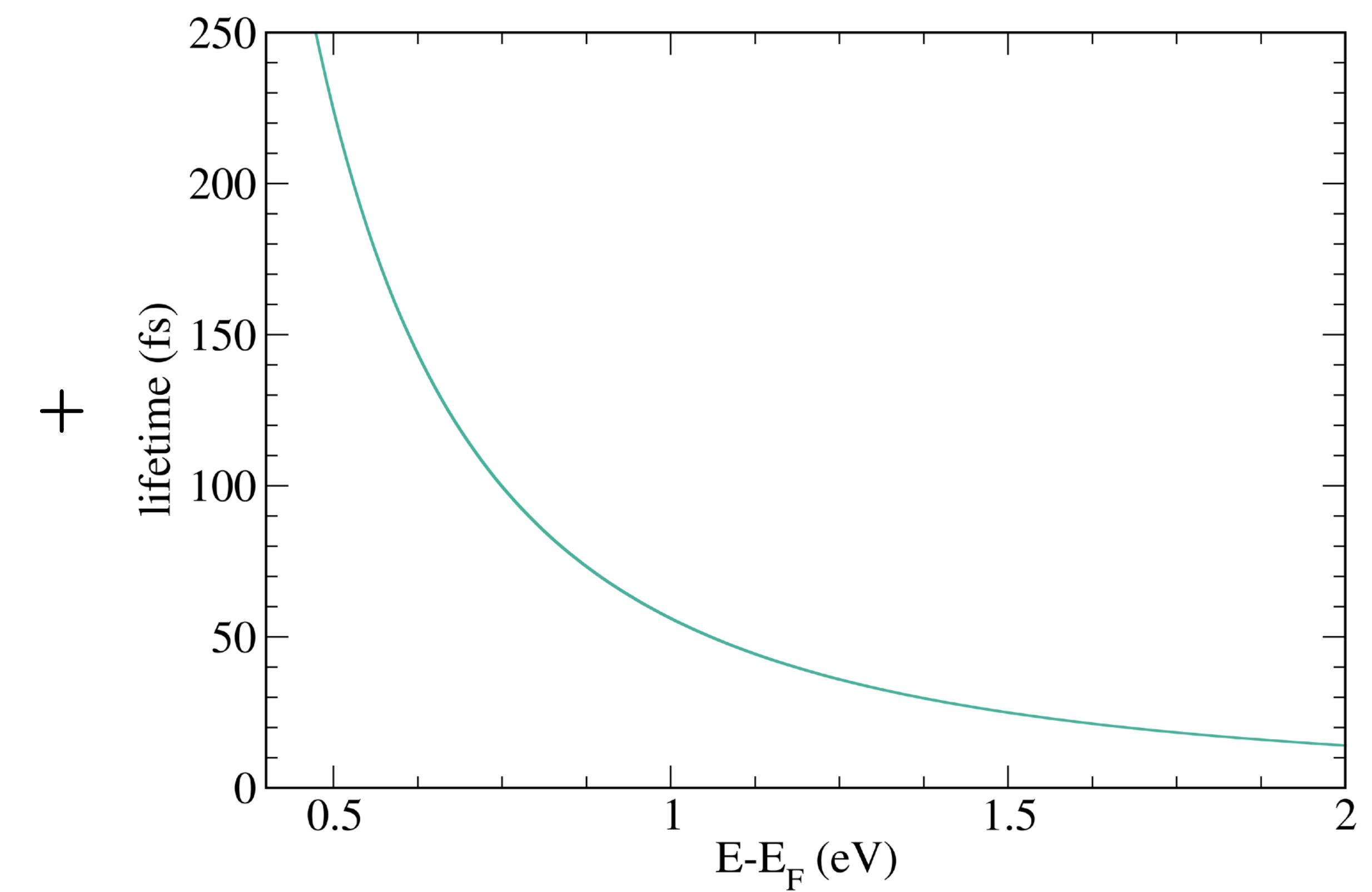
Brief aside away from equilibrium

Toward full relaxation dynamics

Big goal: first principles simulation of equilibration after an ultrafast laser pulse



(Left) Dynamics of electron-phonon driven relaxation in solid beryllium, using PERTURBO

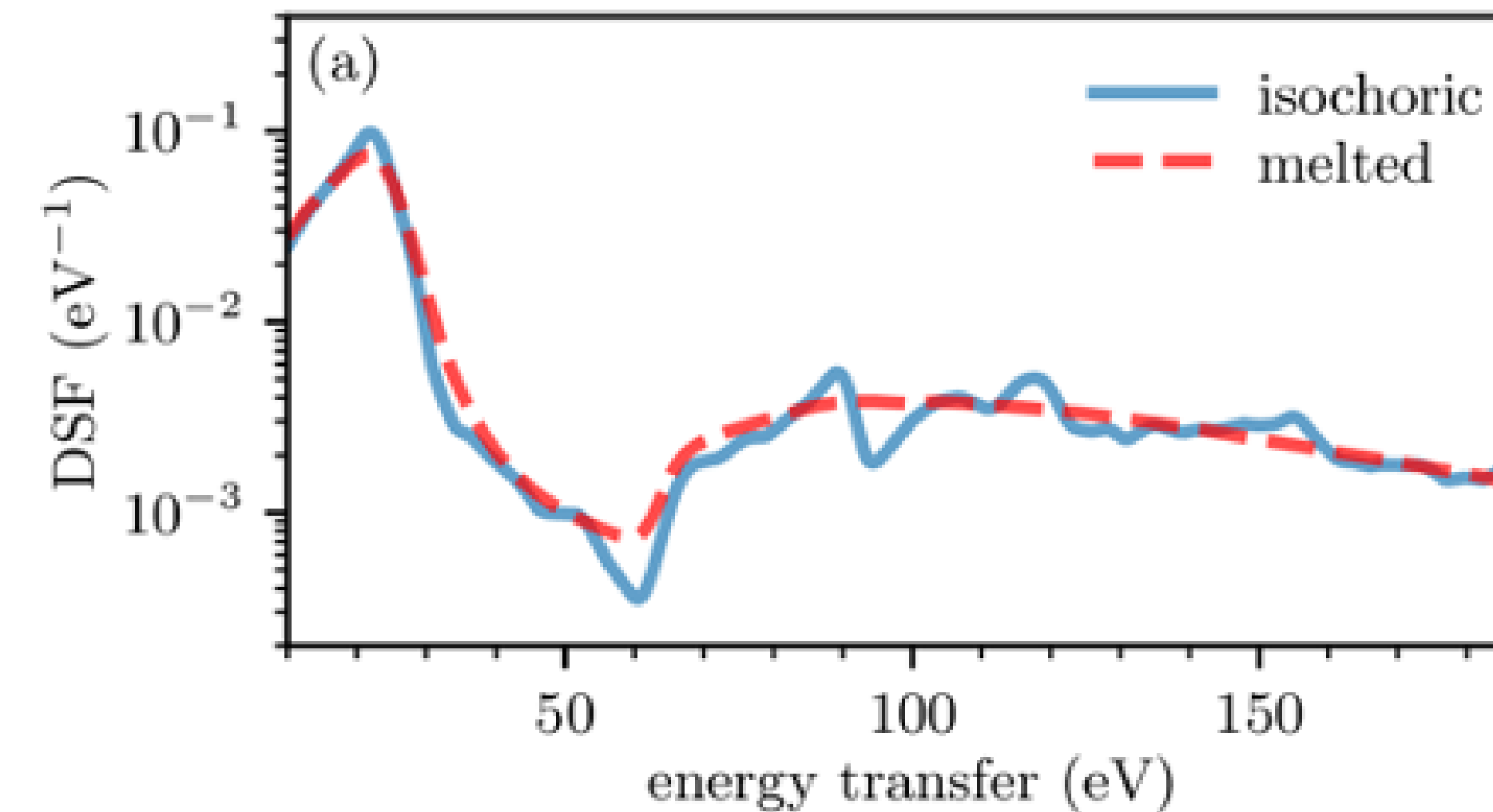
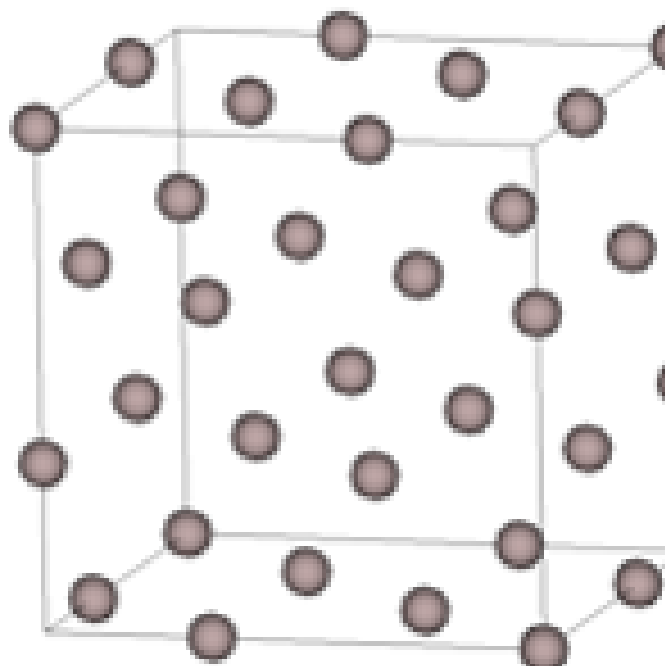


(Right) Fit of G_0W_0 lifetimes for solid beryllium to Landau-Fermi liquid theory

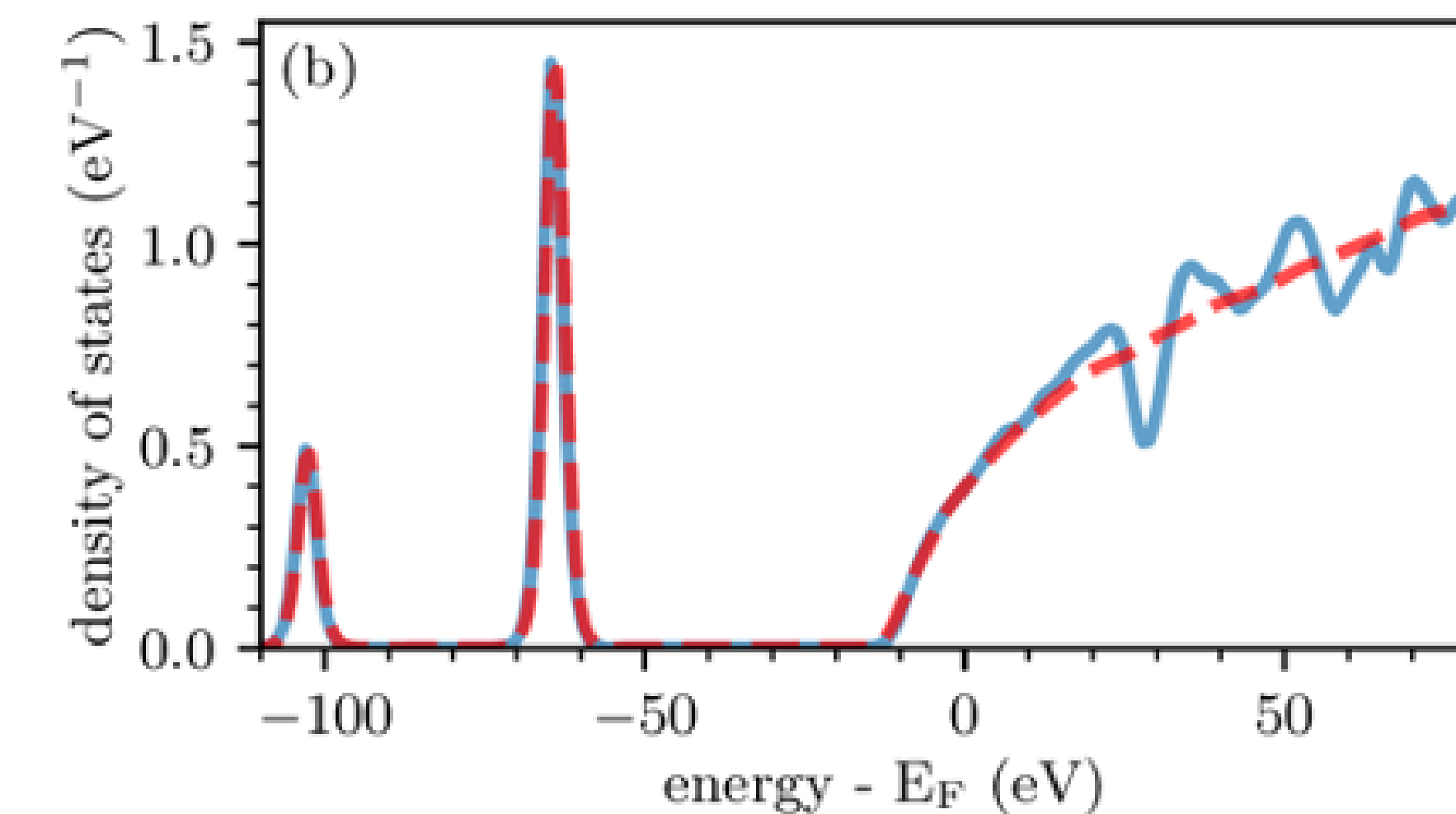
Signatures of non-equilibrium in XRTS

Band structure effects persist for hot electrons that aren't equilibrated with the underlying ions...

Isochoric



Melted



Conclusions

Check out arXiv:2109.09576, preprint on bound-bound results. E-mail is adbacze@sandia.gov.

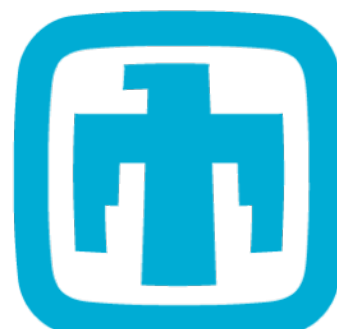
Experimental design and macroscopic simulations require wide-ranging materials models.

Where multi-atom models are too expensive, average-atom models can step in.

We have inclinations about where AA models need refinement and TDDFT corroborates these.

We proposed a metric for determining typicality of trajectories for many-atom stopping, discrepancies between AA and TDDFT seem to be due to collisional models.

Augmented AA theory w/rigorous extension of established scattering theory and partitioning techniques common in opacity to account for bound-bound scattering, consistent w/TDDFT.



**Sandia
National
Laboratories**

Sandia National Laboratories is a multi-missions laboratory managed and operated by National Technology and Engineering Solutions of Sandia, LLC, a wholly owned subsidiary of Honeywell International Inc., for DOE's National Nuclear Security Administration under contract DE-NA0003525.

 **CCR**
Center for Computing Research